EVALUATION OF THE NUCLEAR FIRE THREAT TO URBAN AREAS

Steve J. Wiersma, et al

Stanford Research Institute

Prepared for:

Defense Civil Preparedness Agency

September 1973

Unclassified

SECURITY CLASSIFICATION OF THIS PAGE (When Data Entered)

AD-779 340

REPORT DOCUMENTATION PAGE

READ INSTRUCTIONS BEFORE COMPLETING FORM

1. REPORT NUMBER

2. GOVT ACCESSION NO.

3. RECIPIENT'S CATALOG NUMBER

4. TITLE (and Subtitle)
Evaluation of the Nuclear Fire Threat to Urban Areas

5. TYPE OF REPORT & PERIOD COVERED
Annual Report
8-72 to 9-73

6. PERFORMING ORG. REPORT NUMBER

7. AUTHOR(s)
Steve J. Wiersma and Stanley B. Martin

8. CONTRACT OR GRANT NUMBER(s)
DAHC20-70-C-0219

9. PERFORMING ORGANIZATION NAME AND ADDRESS
Stanford Research Institute
333 Ravenswood Avenue
Menlo Park, CA 94025

10. PROGRAM ELEMENT, PROJECT, TASK AREA & WORK UNIT NUMBERS
2561A

11. CONTROLLING OFFICE NAME AND ADDRESS
Defense Civil Preparedness Agency
The Pentagon
Washington, D.C. 20301

12. REPORT DATE
September 1973

13. NO. OF PAGES
131

14. MONITORING AGENCY NAME & ADDRESS (if diff. from Controlling Office)

15. SECURITY CLASS. (of this report)
Unclassified

15a. DECLASSIFICATION/DOWNGRADING SCHEDULE

16. DISTRIBUTION STATEMENT (of this report)
Approved for Public Release; Distribution Unlimited

17. DISTRIBUTION STATEMENT (of the abstract entered in Block 20, if different from report)

18. SUPPLEMENTARY NOTES

19. KEY WORDS (Continue on reverse side if necessary and identify by block number)
nuclear fire threat, dynamic behavior of fires, structural fire behavior, attack environment following a nuclear detonation, structural response to blast waves, fire spread in debris, simulating air blast effects, blast-fire interaction, influence of air blast.

20. ABSTRACT (Continue on reverse side if necessary and identify by block number)

The nuclear fire threat to urban areas was evaluated in a four-task program. During three previous years of experiments the dynamic behavior of fires in full-scale structures and the nature and magnitude of behavioral changes that result from variations in both structural and environmental factors were studied. This year an

DD FORM 1 JAN 73 1473
EDITION OF 1 NOV 65 IS OBSOLETE

Unclassified
SECURITY CLASSIFICATION OF THIS PAGE (When Data Entered)

19. KEY WORDS (Continued)

20 ABSTRACT (Continued)

attempt was made to integrate the present structural fire behavior knowledge with blast knowledge and to predict the combined blast-fire responses of an urban area to a nuclear attack.

In Task 1 a problem definition and sensitivity analysis was conducted to identify the blast damage and fire situations that are important to study and then a description of an attack environment following a nuclear detonation was attempted. Further analysis of the structural response to blast waves and of the interaction between blast and fire is found necessary before a reliable description of the attack environment can be accomplished.

In Task 2, three field tests of fire development in full-scale structures were made in response to questions raised in the problem definition. In the first field test fire was found not to spread to the interior of a building from a neighboring burning structure so rapidly as expected because induced air currents were drawn toward the initial fire. In the second and third field tests the environment in an improvised basement shelter beneath a burning building and the fire spread in debris were measured.

In Task 3, a method of simulating air blast effects on structures was investigated. The scale model experiment showed promise for simulating room filling by a blast wave; however, simulating the collapse of a structure by a blast wave using the vacuum-air bag technique is not feasible.

In Task 4, a blast-fire interaction experiment was attempted to determine the influence of air blast and its effects on the incendiary responses of combustible target areas. At Mixed Company, a 500-ton TNT blast and shock experiment, test plots of burning liquid fuels contained by a series of pans of varying lengths were located at each of three stations at 5-, 2-, and 1-psi peak overpressures. It was anticipated that the flames on some of the smaller pans would be displaced sufficiently by the shock wave to extinguish the flames, but that the larger pans at each station would remain burning and thus the dependence of the size of threshold fires that are extinguished by air shocks on characteristics of shock and flow could be computed. However, no fire at any of the three stations was extinguished by the shock wave, a result that seemingly contradicts the conclusion of a previous experiment.

ACKNOWLEDGMENTS

Appreciation is extended to the many people who contributed to this research effort, particularly to Raymond S. Alger and his Naval Ordnance Laboratory Group, in residence at SRI, for their suggestions and cooperation, and to Carl Wiehle, John Rempel, and Cecelia Smith for their help in evaluating the structural response of buildings.

ADMINISTRATIVE INFORMATION

The purpose of this task order is to continue the research conducted under Work Unit 2561A of Contract No. DAHC20-70-C-0219 at Stanford Research Institute. The subject matter of this fourth annual report is a portion of the overall objective of the task order, which says:

> "OBJECTIVE: To define through a series of interrelated field tests the nature and magnitude of the nuclear weapon thermal and fire threat to U.S. urban areas."

Based on the task order, a work plan, dated November 29, 1972, was submitted to DCPA for approval. This work plan was accepted by the technical representatives of DCPA.

One task in the work plan called for continued exploratory investigation of the mechanics of air shock extinguishment of flaming combustion using the shock tube facility being built at Camp Parks under Contract No. DAHC20-72-C-0406. Since the shock tube facility was not completed in time to be used during the contract period, the task was dropped from this year's program.

During the contract period, an opportunity arose to study the potentially relevant mass fire hazard in the Oakland hills caused by frost-killed eucalyptus trees. Permission to participate in this study was granted verbally by the DCPA Contracting Officer's Technical Representative, but no formal modification of the contract was deemed necessary.

With the publication and distribution of this report, all contractual requirements are satisfied.

CONTENTS

ILLUSTRATIONS

TABLES

Annual Report *September 1973*

EVALUATION OF THE NUCLEAR FIRE THREAT TO URBAN AREAS

By: STEVE J. WIERSMA and STANLEY B. MARTIN

Prepared for:

DEFENSE CIVIL PREPAREDNESS AGENCY
THE PENTAGON
WASHINGTON, D.C. 20301

CONTRACT DAHC20-70-C-0219
DCPA Work Unit 2561A

SRI Project PYU-8150

This report has been reviewed in the Defense Civil Preparedness Agency and approved for publication. Approval does not signify that the contents necessarily reflect the views and policies of Defense Civil Preparedness Agency.

Approved by:

NEVIN K. HIESTER, *Director*
Materials Laboratory

CHARLES J. COOK, *Executive Director*
Physical Sciences Division

SUMMARY

A. The Problem

In the early transattack period following the detonation of nuclear weapons in and near urban areas, the successful defense of the surviving civilian population and its resources will be determined largely by how securely the population can be sheltered and how effectively certain critical emergency operations can be performed. In this environment, a major continuing threat to the sheltered population and a potential constraint on emergency operations is fire--isolated fires in critical structures, fires spreading into critical areas, fires in residences with basement shelters, scattered fires, group fires, and mass fires.

A great deal is known about the fire-starting capability of nuclear detonations. Much has also been learned in the past few years about how single structures burn. The response of structures to the air blast of a nuclear detonation has also been studied, but little is known about how the blast response of a structure will interact with the fire response of that structure and what synergistic effects will occur in the critical early transattack period following a nuclear detonation.

It has been possible to determine some of the dynamic characteristics of full-scale building fires from experimental burns and from these data to make some predictions about the problems associated with fires following a nuclear attack. But reliable information on the interactive effects of the air blast associated with a nuclear detonation with the fire is more difficult to obtain. An air blast can be experimentally simulated only on a much smaller scale than a nuclear weapon air blast; therefore to

determine experimentally the blast and fire interactions, valid models of structural fire and structural blast effects must be devised and combined.

B. The Findings

Four tasks were performed in our attempts to integrate the present knowledge of structural fire behavior with the knowledge of blast behavior so that the combined blast-fire response of an urban area to a nuclear attack can be predicted.

1 Task 1

The first task of conducting a problem definition and sensitivity analysis to identify the blast damage and fire situations that are important to study and then to describe the attack environment following a nuclear detonation was not so straightforward as first expected because previous blast response studies looked primarily at responses only up to the onset of structural collapse. The purpose of these studies was to evaluate existing structures as shelters, but many of the anticipated fire problems occur at over-pressures higher than those that initiate structural collapse. In a preliminary study of blast-fire interaction problems, four areas of concern were identified:

(1) The fire problems expected are very dependent on the self-help response of the people, and the response depends to a critical degree on preattack planning and training.

(2) The spread of fire between buildings is important, and and the chronology of the development of this type of fire needs to be better known.

(3) The effect of the blast wave in blowing out or spreading fires ignited by the thermal pulse needs to be better understood.

(4) The dependence of debris-fire behavior and rates of spread on the significant variations of debris characteristics needs experimental attention.

Much of our effort to describe the attack environment following a nuclear detonation was spent in extending and applying blast response data and blast-evaluating techniques to areas pertaining to fire problems. A computer program developed by Longinow of IITRI, which follows the path of blast-translated debris was modified so that we could predict the final distribution of debris from a collapsed structure. An attempt to characterize the structural responses to air blast loading in nondimensional parameters, and thereby improve damage assessment capabilities was also begun. The response of a hypothetical urban target synthesized from buildings whose blast vulnerability had been previously evaluated for specified attack situations was developed to the point where we could plainly see what further analysis of the structural response to blast waves and of the interaction between blast and fire would be needed before a reliable description of the attack environment could be made.

2. Task 2

In the second task three field tests of fire development in full-scale structures were made in response to questions raised both in the problem definition and about the vulnerability of an improvised shelter in a basement to a fire in the building above the shelter. The first experiment showed that fire did not spread to the interior of a building from a neighboring burning structure so rapidly as expected because of air currents induced toward the initial fire. Airflow patterns have a critical influence on rates of fire spread and fire development. The second experiment showed that a basement shelter constructed by piling soil on the floor of an existing building was not well protected from a fire in the building, particularly from the toxic combustion products of the fire. An important observation in the third experiment in which the fire spread into debris, was the difference in upwind and downwind modes of fire spread in the debris. Downwind the fire spread

along the top surface of the debris and a substantial amount of material burned well behind the fire front. Upwind the fire spread within the debris and all flaming combustion occurred within five feet of the fire front.

3. Task 3

A method of simulating air-blast effects on structures was investigated in the third task. The air pressure on the interior of a scale model building was reduced below atmospheric pressure. The windows of the building were then broken, which allowed outside air to fill the partial vacuum. Airflow through the openings was hypothesized to be similar to the airflow following a blast wave hitting the building. The scale model experiment showed promise for simulating room filling by a blast wave. However, our scale model experiment showed that it would be very difficult to simulate the collapse of a structure by a blast wave by creating a vacuum in the interior of the structure and then breaking critical structural support members.

4. Task 4

The fourth task was an experiment to determine the dynamic influences of the passage of an air shock over ignited materials. From the experiment, which was done at Mixed Company, a 500-ton TNT blast, we had hoped to determine the limiting size at which "blowout" of flaming combustion occurs and how this limiting size varies with the characteristics of the shock. It was hoped that the range of fire size at each of the three different peak overpressure locations would permit at least one fire to be extinguished and at least one fire to survive the passage of the shock wave. However, no fire at any of the three stations was extinguished by the shock wave. The shock wave did not create a shearless displacement of the flames from the fuel, as had been postulated to occur.

5. Supplementary Study

In a supplementary study (approved by DCPA) we were asked to help evaluate the fire hazard from freeze-killed eucalyptus trees in the San Francisco Bay Area. Our experimental measurements showed that the ease of ignition and the burning rate of freeze-killed leaves were much greater than those of naturally-dried leaves. This information helped establish the conclusion that there indeed was an extraordinary fire hazard. Because of the extraordinary fire hazard the affected communities took action to lessen the potential danger.

I INTRODUCTION

The fourth year of the structural fire dynamics program changed emphasis from primarily establishing the burning behavior of wood-frame structures, as was done in the first three years of the program [1,2,3] to (1) integrating the present structural fire behavior knowledge with the blast behavior knowledge so that the combined blast-fire response of an urban area to a disaster, particularly a nuclear detonation, can be predicted; (2) determining the information gaps in the combined blast-fire response knowledge; and (3) beginning to fill these gaps.

The first task of this year's program was to conduct a problem definition and sensitivity analysis to identify the blast damage and fire situations that are important to the study and then to describe the attack environment following a nuclear detonation. The situations of most interest are those in which there is a high concentration of persistent fires, yet most of the population survives the other direct effects and is capable of fighting the fires.

The second task was to continue fully instrumented field tests of fire development in full-scale structures. These experiments were to be designed to respond to questions raised in the problem definition. Three tests were conducted: the first observed the influence of a fire in an already burning building on a second building close enough to the first so that fire spread to it was virtually assured, the second experiment tested the influence of a structural fire on the environment of an improvised shelter below the building, and the third observed the fire spread through a debris pile. The first two of these tests used Camp Parks barrack sections identical to those used in the past three years.

For the third task a scale-model house was used to investigate the feasibility of using full-scale structures for blast-fire relevant tests. The dynamic shock effects of a nuclear detonation associated with room filling were simulated by rupturing the pressure-tight envelope at the windows on one side of a building in which a partial vacuum had been drawn. Attempts were also made, unsuccessfully, to duplicate the dynamics of collapse.

The fourth task was undertaken to explore other approaches and other potential sources of information relevant to the blast and fire problems that are expected to follow a nuclear attack. An opportunity to investigate the dynamic effects of the passage of an air shock over ignited materials was afforded by the Mixed Company Event, a 500-ton TNT blast and shock experiment. An experiment was performed that had the goal of relating the dependence of threshold fire sizes that are extinguished by classical waveform air shocks on such characteristics of the shock and flow as peak overpressure and positive-phase duration.

A fifth task of the program was to use the shock tube facility under development at Camp Parks to investigate in detail the mechanisms of fire blowout. However, the construction of this facility was not completed in time for use in this contract year. Therefore, alternative additional work was undertaken in other tasks. For example an opportunity to study a potentially relevant fire problem occurred in the East Bay hills eucalyptus tree crisis. Large areas of frost-killed trees had created a potential mass fire hazard. Because of our previous studies for DCPA of mass fire problems, we were able to assess the potential fire hazards and recommend preventive action. The results of this study materially aided in the decision by the Office of Emergency Preparedness about Federal intervention and assistance in the face of the threat.

We also participated in two other fire experiments. The first measured the thermal radiation and carbon monoxide concentration at a prescribed wild land fire. The second evaluated a fire retardant emulsion for protecting hills-area structures from wildfires.

This report summarizes the results of the fourth year's study of structural fire dynamics conducted by Stanford Research Institute in cooperation with the resident Fire Research Group of the Naval Ordnance Laboratory. Each task of the program is sufficiently independent to warrant separate sections for background, experimental, results, and conclusions. The four tasks are covered in Sections II, III, IV, and V, respectively. Our activity in the eucalyptus tree crisis is reported in Appendix F. The two fire experiments using wild land fuels are described in Appendix G.

II IDENTIFYING THE BLAST DAMAGE AND FIRE RESULTING FROM NUCLEAR DETONATIONS

A. Background

Our previous studies of structural fires[1,2,3] have concentrated on fires in buildings that were only slightly damaged. In most cases the buildings had only broken windows and opened doors which simulates building damage from a shock wave with less than roughly a 1/2-psi overpressure. It became apparent when we reviewed other studies made for DCPA that fires in structures with damage resulting from shockwaves of greater overpressures may be at least as important to study as those we were studying. Therefore, we attempted to describe the nature of fires in buildings effected by varying degrees of blast damage, and then to define the areas in which it is most important to know the dynamic characteristics of the fires, that is, to define the areas where fires would be prevalent following a nuclear attack but could be controlled.

Predictions have been made on the blast response of structures in a nuclear attack,[4,5,6] on the safety of people in a direct-effects nuclear weapon environment,[7,8] and on the number and types of fire starts caused by a nuclear burst,[9,10,11] but an integration of predictions from these areas that would define the most important fires that need to be studied has not been attempted since 1967, before the interactions of blast and fire in urban enclosures were studied by Goodale et al.[9,11]

B. Problem Definition

We conducted a preliminary study in which we used the predictions of the blast response,[4,5,6] the safety of people,[7,8] and the fire starts,[9,10,11] to identify areas of concern. Our first finding was that the fire problems expected in the event of a nuclear attack are very dependent on the self-help response of the people and that the response depends to a critical degree on preattack planning and training. For

example, areas that experience roughly a 2-psi maximum overpressure shock wave from a megaton yield explosion will have very few room fires that will develop to flashover, but these very few fires could lead to a mass-fire situation if they are not attended to in less than one-half hour after the blast. However, if preattack planning has placed building monitors in all buildings and they are trained to detect and extinguish these fires quickly, fire problems in such areas will be minimal.

Our second finding of the preliminary study was that in areas in which blast overpressures are below about 1 psi and in cases where visibility is below 5 miles and blast overpressures are below about 2 psi, there will not be an initial mass-fire situation in which many buildings burn simultaneously from fires ignited by the thermal pulse. If a mass-fire situation develops, it will be caused by fires that have spread from the occasional building that was ignited by the thermal pulse of the explosion or from secondary causes. Therefore, interbuilding fire spread is important, and the chronology of such fire development needs to be better known.

Our third finding was that the effect of the blast wave on fires ignited by the thermal pulse needs to be better understood. Two studies have been made to assess the effects of the blast wave on fires, the first study was made in a large shock tunnel[8,11] and the second was our field test at Mixed Company, described in Section V of this report. The findings of the two studies are inconclusive on what types of fires can be expected to be blown out by the blast wave. The fire problems that can be expected in a nuclear attack are very dependent on the blast wave blowout predictions.

The fourth area of concern was debris-fire behavior. There is very little information on the behavior of fire in debris resulting from a nuclear explosion, and many fire starts will occur in areas where structures are reduced to debris. Therefore, we believe that some early

experimental attention should be given to assessing the dependence of debris-fire behavior and rates of spread on the significant variations in debris characteristics.

C. Description of Urban Damage Following Nuclear Attack

To gain further insight into the interactive effects of blast and fire and to ascertain the extent to which the present state of the art permits the details of the component effects to be estimated individually, we initiated an analytical study of the damage responses of typical urban areas. The goal of this study is a series of detailed illustrations with narrative descriptions of the immediate postdetonation state in one or more representative urban use-class areas that would result from varying levels of damage. The damage levels of interest range from insignificant damage to nearly complete destruction--or at least to the point where the damage is so severe that little more of value to civil preparedness can be learned by attempting to analyze situations of heavier damage. This point of diminishing returns has been reached, then, when few survivors remain who either can help themselves or can be helped, when debris becomes so excessive that other emergency operations are impossible to perform, or when all fire-blast phenomena and their interactions that can affect the overall threat of fire in less severely damaged areas have been evaluated.

1. Procedure

We thought damage response could be described using current data if the urban area to be analyzed were composed of structures whose blast-response vulnerability had already been ascertained, if the condition of the explosion were specified in detail, and the target/attack geometry were selected to provide somewhat idealized weapon effect loading on the structures. Accordingly, a hypothetical urban area was synthesized from

structures drawn from a recent all-effects survey and analysis, and this model area was to be subjected analytically to a specified set of attack conditions. Results of the structural analyses of Wiehle and Bockholt[5,12] were to be used to evaluate the collapse of structural elements. Debris distributions were to be estimated using the computer program recently developed by Longinow.[13] Estimates of the incidence and distribution of fire starts were to be made using an updated version of the URS model developed by Martin and Ramstad. (See Appendix D)

The synthesis of the model target is described and the various attack situations are specified in Appendix A. Appendix B presents a basic exposition of the interaction of air blast with structures and the responses of structural components to air blast loading. In developing this material we recognized the importance of making generalizations to the fullest practical extent, and we attempted, with considerable success, to derive nondimensional relationships governing the mechanics of loading and response. These derivations represent a significant contribution to the subject because they provide the basis for scaling laws that (1) can be employed to design physical models for experimental study of blast-fire interactions; (2) will allow the rigorous evaluation of parametric sensitivity; and, perhaps most importantly, (3) will provide physical insight into the processes involved.

The Longinow debris program was modified to increase its utility and convenience of use. The modified program is described in Appendix C, and example results of its use are included. Finally, to minimize the manual effort entailed in estimating initial fire incidence with the URS fire-start model, a time-share computer program was written to permit machine computation. This program is reproduced in Appendix D.

2. Results

The results of the analysis of the specified weapon effects on the hypothetical area were seriously limited by the state of the art of blast damage assessment. The principal limitations lie in two areas:

(1) Lack of knowledge about the details of the breakup of structural elements for blast loadings that appreciably exceed the incipient collapse values.

(2) The fate of initial fires disturbed by strong shock waves that may either blow the fires out or drastically redistribute the fuels in which the fire will grow and spread if not blown out.

In the first of these two it is particularly noteworthy that structural damage analyses of specific buildings, such as the ones selected here to synthesize the hypothetical urban area, have to date focused their attention on designating incipient collapse overpressures for exterior walls because the analyst has been preoccupied with problems of rating shelter vulnerability. Some limited attention has been given to interior walls, structural frame members, and even to the integrated response of an entire structure; nevertheless, little attention has been given to describing the response (and resultant state) of structural elements and whole structures (not to mention contents) when they are mechanically loaded by overpressures substantially exceeding the threshold values for collapse. Some sensitivity studies* that concentrate on specific situations rather than attempting to generalize have produced some interesting relationships to indicate the dependence of such important response descriptors as the time of collapse, the sizes of fragments, and the initial velocities of fragments on the characteristics of the blast wave--notably, its peak overpressure

*Reference 12 contains an example.

and how much it exceeds the incipient collapse overpressure of the wall panel or other structural element in question. But these relationships are of limited use because they lack generality, having been derived for a few specific cases only. In our initial approach to damage description, we attempted to circumvent the need for generalizable methods of analysis by synthesizing the hypothetical urban area out of structures for which blast response calculations had been made previously. In this we were thwarted because of the nature of the prior calculations, as already noted, and were forced to devote an appreciable part of our effort (see Appendix B) in attempting to scale the relationships that are needed to make the necessary extrapolations. These efforts were not rewarded by success in the solution of the short-term problem, but, and far more importantly, they were rewarded by the development of a methodology from which a substantially improved damage assessment capability can soon emerge.

The modified Longinow debris model performs successfully; it gives useful deterministic estimates of the trajectories and final location of objects of specified geometry and specified initial conditions. To the extent that the results are applicable to the present problem, they are deficient in several respects. A major weakness is in the description of breakup and specification of conditions at the moment of collapse. As noted above, we are usually unable to extrapolate the blast responses of structural elements sufficiently to provide an adequate description of the initial condition and the state of debris particles. Another unsatisfactory aspect of applying the Longinow debris model to the problem at hand is inherent in the model's deterministic character. It is manifestly unrealistic to attempt to describe any "real world" debris situation in anything but a random distribution or some similar stochastic form. On the other hand, the deterministic debris model steadfastly avoids any treatment of randomizing processes and computes each particle's motion without reference to any other nearby particle that may be in motion at the same

time. Even the effects of distributed properties of many particles in the total population, which would lead to a distributed solution if a very large number of sample calculations were run, cannot be taken into account until input statistics have been established. Thus we can only explore the sensitivity of the results to the input variables in anticipation of a fuller understanding of how the initial state of debris depends on the blast wave that generates it. This we have done in a preliminary way and reported in Appendix C.

3. Conclusions

Considerably more work needs to be done on the analysis of mechanics of structural response to blast waves and on the interactions between blast and fire before a reliable description of the attack environment can be accomplished. Also, the debris model must have input data over the range of likely conditions before its results can be interpreted satisfactorily.

III FIELD TESTS OF FIRE DEVELOPMENT IN FULL-SCALE STRUCTURES

A. Background

Two field tests were conducted in response to the initial problem definition of Task 1, and a third test was conducted in response to questions raised about basement shelters at the Annual DCPA Fire Research Contractors Conference.

One of our findings of Task 1 was that fire spread between the buildings is a crucial factor in determining if a mass-fire situation will develop in the event of a nuclear attack. Our first field test this year looked at the sequence of development of a fire that was ignited in one barracks building and spread naturally to a neighborning building located downwind from the first building. We had previously conducted two tests[2] in which two buildings were burned together, but in each test the two buildings were ignited at the same time and the wind direction was such that it tended to maintain two separate fires and not to blow the flames of one fire onto the neighboring building. Ignition studies had also been made[2] to determine the times and distances at which redwood siding on one building would be ignited from a fire in another building. But the sequence of fire development in the spread from one building to a second building needed to be determined.

The evacuation of high risk areas in the United States is being considered as a countermeasure to the Soviet Union's plan of evacuating its cities in the face of a nuclear war threat. In the event of the evacuation of many people, it would be necessary to provide many more fallout shelters in the outlying areas to which the people are evacuated. One means of rapidly constructing temporary fallout shelters is to protect

basements of existing buildings from radioactive fallout by piling soil and other shielding media on the floors of the buildings and also mounding up the soil around the buildings to the level of the soil on the floors. Our second field test determined the environment in one of these soil-protected shelters beneath a burning building. The shelter was built with a barrack section similar to those used in past tests. The temperature history and the toxic gas concentrations in the shelter were measured.

In our third and final field test of the year we observed the behavior of a debris fire. One of the areas of concern identified in Task 1 as needing attention was assessing the dependence of debris-fire behavior and rates of spread on the significant variations of debris characteristics. A large pile of wood scraps was available for us to use to observe the rates of spread of fire in one type of debris. This debris fire provided an opportunity for us to observe the fire spread rate in several directions relative to the wind field.

B. Fire Spread Between Buildings--Experiment 13

1. Test Procedures

Experiment 13 was conducted on March 7, 1973. (Experiments 1 through 12 in the structural fire dynamics program were conducted in the first three years of the program and reported on in previous annual reports.)[1,2,3] Two Camp Parks barracks sections were positioned so that the prevailing winds would blow the fire from one building directly toward the second building, which was located 12 feet downwind from the first. The construction details of these buildings were described in our 1970 Annual Report.[1] Both buildings were furnished like those in Experiments 10 and 11:[3] noncombustible gypsum board ceilings that delay fire spread between the rooms and attic replaced the Celotex ceilings of

the original buildings, and three pounds per square foot of furnishings and other combustibles were added to the rooms. The chairs, tables, and desks were made of scrap lumber to simulate wood furniture, but actual beds, sofas, carpets, clothing, and curtains were also used so that fire spread in real homes would be simulated. All windows were broken out and all doors were removed in both buildings so that the situation in this year's burns corresponded to those in the previous years.

An instrumentation diagram is depicted in Figure 1. Instrumentation was similar to that used in previous years.[2,3] Building B, the downwind building, was supported on water-cooled, hydraulic load cells with remotely located electrical transducers to measure weight loss throughout the burn. Eleven radiometers at window level and one radiometer on a 35-foot tower which provided an approximately 45° elevation angle, line-of-sight sampling of the radiation-flux field, measured the irradiance around the buildings. Time-lapse cameras provided a photographic record of the fires. Air temperatures in several rooms of Building B and temperatures of the redwood siding and the shingle roof that faced Building A were measured with chromel-alumel thermocouples. Fire-spread rates were measured within each building by the burning-string method, and the ambient wind velocity was measured.

The blankets and sheets on the bed in Room 1 of Building A were ignited with the help of about one quart of kerosene.

2. Test Results

The measurements taken in Experiment 13 are summarized in Appendix E. The wind velocity fluctuated between 6 and 10 mph from a west-southwest direction during the experiment so that the flames from Building A were blown almost directly toward Building B. During the early period of burning, from 0 to 15 minutes after ignition of Building A, much smoke was blown into Building B from the fire in Building A.

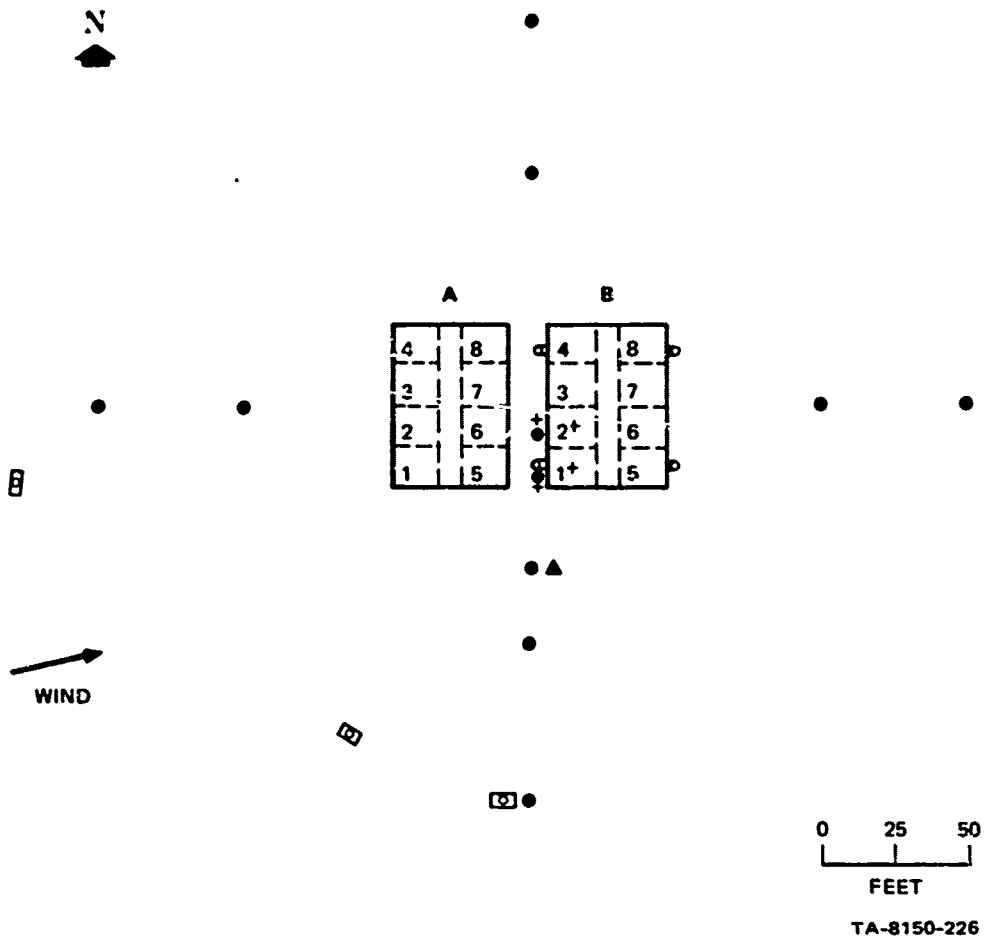

FIGURE 1 INSTRUMENTATION PLAN IN CAMP PARKS EXPERIMENT 13

Building A was ignited in room 1. The instrumentation symbols are: radiometer at window level, ●; radiometer 35 ft above ground, ▲; load cell, ⊟; thermocouple, and time-lapse camera, ⊡.

About 17 minutes after ignition, the flames through the windows and roof of the east side of Building A filled the 12-foot alley between the two buildings and ignited many spots on the redwood siding, the eaves, and the shingle roof on the west side of Building B. As can be seen from the radiant flux measurements of the radiometers that were located flush with the outside wall of Building B pointing toward Building A and from the temperature measurements on the outside walls and roof of Building B as shown in Appendix E, Figures E-3 and E-4, respectively, Building B had received very little thermal energy from the fire until the 17 minutes after ignition. After the flames from Building A had filled the alley between the buildings for about one minute, thoroughly igniting the outside of Building B, the flames of the Building A fire retreated. Inflow winds created by the Building A fire were strong enough to draw air from the alley between the buildings and even create airflow through Building B toward Building A in the opposite direction to the ambient wind. This airflow was sufficient to remove from inside Building B almost all of the smoke, which earlier had been dense enough to require observers in Building B to leave at 10 minutes after ignition time. Several curtains on the west windows of Building B had been ignited during the 17 to 18 minutes after ignition; these curtain fires might have been sufficient to ignite other furnishings had the airflow carried them into the rooms, but the airflow from inside to outside made these curtain fires relatively harmless. Escape from these rooms would have been possible until about 35 minutes after ignition of Building A, as shown by the room air temperature measurements in Figure E-4 in Appendix E.

There was a period of almost 20 minutes from the time the outside of Building B was ignited until fire entered any of the rooms in the building. We had thought that the combustibles inside the rooms--the beds, sofas, and clothing--would ignite from radiant exposure at about the same time as the redwood siding of the building, but this was not the case.

Building A slowed the growth of fire in Building B because of the airflow created by the Building A fire.

The two buildings burned almost independently. Building A had completely collapsed 35 minutes after ignition, which was before the fire flashed over to any of the rooms of Building B. There were two distinct radiant energy pulses, as can be seen in Figure E-2, Appendix E. The first maximum occurred about 23 minutes after ignition when Building A reached its maximum burning rate, and the second occurred about 50 minutes after ignition when Building B reached its maximum burning rate. The values of t_{max}, the time after ignition to maximum burning rate, and t_c, the interval of time that the burning rate is greater than the half-maximum burning rate (which we previously used to compare the different experiments[3]), are t_{max} = 23 min and t_c = 14 min for Building A. These values correspond very closely to the values found for Experiments 10 and 11 in which buildings were burned under similar conditions.[3] For Building B, t_c = 12 min, but t_{max} is not defined because the building was not ignited in the same way as the other buildings. The maximum burning rate of W_{max} = 5100 lb min^{-1} for Building B is a very high burning rate compared with those previous experiments, which implies that a large portion of Building B was burning at the time of maximum burning rate. The fact that 6 of the 8 rooms of Building B recorded string breaks within a 2-minute period of time in the fire spread measurement, as shown in Table E-1 in Appendix E, is further indication that a large fraction of the building was vigorously burning at the same time and that the fire spread very rapidly through the building once it entered the interior of the building.

C. The Environment in an Expedient Soil-Protected Shelter Beneath a Burning Building--Experiment 14

1. Test Procedures

A simulated fallout shelter was built beneath one of the Camp Parks barracks sections by first strengthening the supports beneath the structure and then covering the floor in the building with a minimum of one foot of soil and gravel and mounding soil and gravel around the edges of the building to the level of the material on the inside floor. A photograph of the building is shown in Figure 2. The soil that was scraped from around the building contained much clay so it remained in large chunks and was very difficult to spread. Therefore, sand and gravel were spread over the chunks of soil to fill the void spaces. The sand and gravel mixture consisted primarily of pea-sized stones and fine sand; it filtered into the void spaces between the chunks of soil very easily and was easy to spread, providing a uniform surface.

The shelter area beneath the building was about 38 feet wide, 48 feet long, and 3 feet high. Gas composition was sampled at two locations, one in the center and the other in the downwind, northeast corner of the shelter. The CO, CO_2, and O_2 concentrations were continuously measured with commercial analyzers throughout the fire. The temperatures were also measured at each sampler location with chromel-alumel thermocouples.

The ceilings were not modified with gypsum board; the original Celotex ceilings remained. Three pounds per square foot of scrap lumber was placed on the soil in the rooms to provide a fuel loading similar to the fuel loading of furniture in a house; however, no sofas, beds, clothing, or curtains were used.

The fire on the morning of April 28, 1973, was monitored by 10 radiometers placed around the building at locations used in past experiments

(a) BUILDING BEFORE FIRE

TA-8150-227

(b) BURNING BUILDING

FIGURE 2 PHOTOGRAPHS OF THE SOIL-PROTECTED SHELTER AND BUILDING IN EXPERIMENT 14

so that the intensity of the fire could be compared with that in the other experiments. Ambient wind velocity was also measured.

2. Test Results

The building fire in this test had a t_{max} = 18 min and t_c = 12 min, both of which are less than the values for experiments with similar building conditions like Experiments 1, 2, or 8,[3] and indicate a shorter and more intense fire in this experiment. However, the maximum radiant fluxes shown in Figure E-5 in Appendix E are similar to those of previous tests. A smaller amount of fuel was available for the fire in this experiment than in earlier ones because part of the fuel was protected by the soil from the fire. Hence, it is possible for the characteristic burning time, t_c, to be less than that in previous burns and yet for the maximum burning rate, to be similar to those in the previous cases.

The wind velocity during the experiment averaged 9 mph from the west. The concentrations of CO and CO_2 in the shelter during the burn are shown in Figure E-6 of Appendix E. The maximum concentrations of CO and CO_2 during the first hour were 0.85 and 5.5 percent, respectively. Although there were two sampling locations, one in the center and the other in the northeast corner of the shelter, only one could be analyzed at a time. However, the plot of the concentration of CO and of CO_2 appears to be almost continuous even when we switched from one sampling location to the other, which suggests that there was sufficient mixing to provide an almost uniform concentration of combustion product gases throughout the shelter. We also measured a decrease in O_2 concentration from 21 to 19.5 percent during the burn. The oxygen depletion is almost totally caused by the displacement of air with CO and CO_2 and is not caused by oxygen from the shelter being used in the combustion. The temperature in the shelter increased only very slightly during the first hour after ignition. Ambient temperature in the shelter was 20° C before ignition;

there was no measurable increase in the first 30 minutes after ignition, and the temperature was only up to 40°C at the end of an hour.

The most dangerous health hazard effect in the shelter due to the fire in the structure above appears to come from CO. A 1-hour exposure of 0.2 percent CO to a person doing heavy work and of 0.35 percent CO to a person at rest is enough to cause death.[14] The measured levels of CO would cause loss of consciousness to persons housed in the shelter in less than 25 minutes after ignition. The concentrations of CO_2 measured in the shelter would not be lethal by themselves but would cause a markedly increased respiratory effort that could quicken the toxic effect of the CO. A quantitative measure of this synergistic effect is not currently available for human subjects.[15]

The first detectable CO was measured in the shelter 7 minutes after ignition, which was approximately the same time that the fire moved from the first room to other rooms in the building. We think the combustion gases traveled from the rooms down to the shelter by first entering the dead space in the walls between the two gypsum board surfaces and then filtering through the floor to the shelter. The soil on the floor did not protect the shelter from gases entering by this route. After several hours, fire also entered the shelter by burning down between the walls.

D. Fire Spread in Debris--Experiment 15

1. Test Procedures

We had a large pile of wood scraps available for use in our experiment. The debris consisted almost entirely of discarded lumber from remodeling construction and discarded wooden pallets. A few logs and branches from trimmed trees were spread along the generally downwind edge of the debris, but the primary fire spread measurements were not taken in this area. Figure 3 is a map of the debris. The fire was started

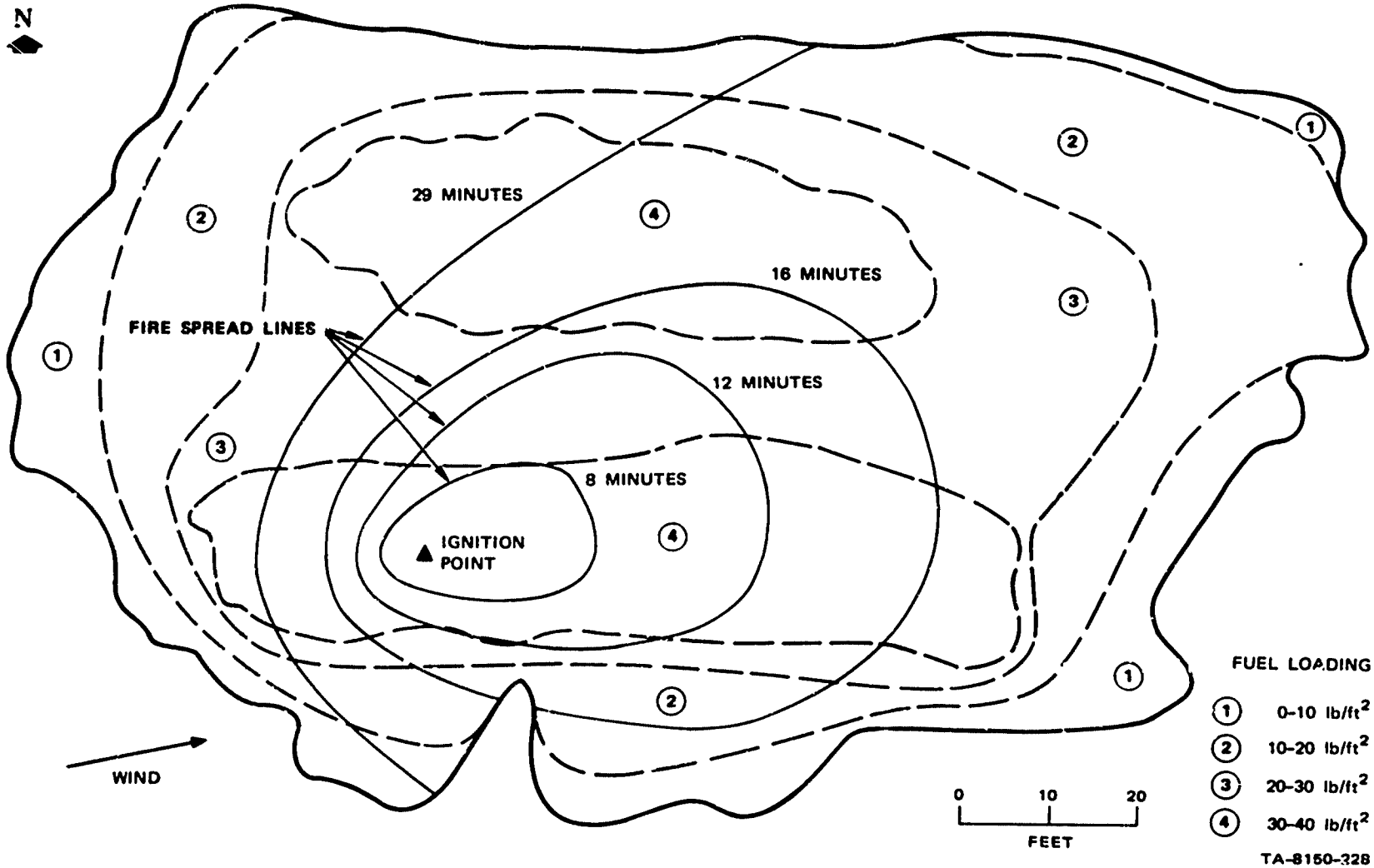

FIGURE 3 FIRE SPREAD IN WOOD DEBRIS IN CAMP PARKS EXPERIMENT 15

about 25 feet from the upwind end of an area approximately 20 by 100 feet that had a relatively uniform fuel loading of 30 to 40 pounds per square foot; consequently, fire spread could be measured both downwind and upwind. The depth of debris in this region was 4 to 5 feet, and the fuel density averaged about 8 pounds of wood per cubic foot.

Time-lapse photography recorded the behavior of the fire. Markers were placed in the debris at various points, and the time that the fire reached each marker was recorded.

2. Test Results

The test was conducted on the afternoon of April 28, 1973, when the wind velocity was 7 mph from the west-southwest, as indicated in Figure 3. Also in Figure 3 are the point of ignition of the fire and the approximated lines to which the fire had spread in 8, 12, 16, and 29 minutes. These fire spread lines were estimated from the time-lapse photographs and also from the visually recorded times at which the fire had reached various marked points

The fire required 6 to 8 minutes to build up the flame height to 10 to 20 feet above the debris. A plot of the linear fire spread rate in both the upwind and downwind directions is shown in Figure E-7 in Appendix E. The three points that were measured for fire spread with the wind show that after 8 minutes the fire spread at a steady rate of about 5 feet per minute. The fire, progressing with the wind, seemed to maintain vigorous burning, with 10- to 20-foot-high flames for 5 or 6 minutes at each point before the flames fell to less than 5 feet above the debris. The fire appeared to spread along the upper surface of the debris, leaving a substantial amount of material to burn well behind the fire front.

The fire spread against the wind at a rate of 0.7 foot per minute as seen in Figure E-7 in Appendix E. The flame heights of this fire were less than 5 feet above the debris. In this case the fire appeared to spread within the debris and then to the surface of the debris.

E. Conclusions from the Field Tests

The results of Experiment 13 were unanticipated. We had thought that the second building would reach its maximum burning rate soon after the building caught fire because we expected the fire spread to be enhanced by radiant energy input from the first burning building. Instead, the fire burned only on the exterior of the second building for a long time because the fire in the first building created sufficient inflow winds to prevent the spread of fire to the interior of the second building, and an interior fire is necessary for high burning rates. T. E. Waterman of IITRI[16] noted a similar phenomenon of an upwind fire decreasing the fire spread rate in a structure toward which the ambient wind was blowing because of airflow produced by the upwind fire. However, he observed that structures must be close together for this phenomenon to occur and that the original fire enhances the fire spread of the second fire when structures are further apart. Our experiment also shows that airflow patterns have a critical influence on rates of fire spread and fire development. This fact creates a frustrating situation because ambient winds cannot be accurately anticipated and local airflow parameters are difficult to predict and to measure in a fire environment.

The results of Experiment 13 also suggest that a mass-fire situation is not likely to develop from fire spreading from an isolated structure in that the fire in Building B in our experiment did not develop quickly enough to be enhanced by the fire in Building A, which suggests that a cascading fire situation that leads to a mass fire might not occur. However, caution must be exercised in extrapolating from two

structures to many structures when airflow patterns are so difficult to predict. Here is an area of inquiry where reliable reduced-scale modeling would be of inestimable value.

The soil-protected shelter beneath the burning building in Experiment 14 did not provide sufficient protection for inhabitants. The soil provided enough thermal insulation to protect the shelter from the high temperatures until the fire actually entered the shelter by burning between the two gypsum board surfaces of the walls and then through the floor. But the soil did not protect the shelter from the toxic combustion products of the fire because combustion products entered the shelter soon after the fire was ignited. The flow of combustion product gases through the floor is probably very sensitive to the type of construction; a concrete slab floor probably would have provided a sufficient barrier to the gases. The Camp Parks barracks had 1- by 8-inch subflooring to which the headers for the wall studs were attached, and the flooring, made partly of hardwood and partly of plywood covered with linoleum, was laid up to the the headers. All this wood did not present a sufficient barrier to the gases.

One of the most interesting observations of the debris fire-spread test, Experiment 15, was the different modes of fire spread in the upwind and downwind directions. The downwind fire spread, which appeared to spread along the top surface of the debris, was probably due to convective and radiative energy being transferred from the flames to the upper fuel surfaces downwind from the fire. A substantial amount of material was burning well behind the fire front. The upwind fire spread, which appeared to spread from within the debris, was slow and all the flames were within five feet of the fire front.

The measured downwind fire spread rate of 5 feet per minute is the same as that measured in Experiment 12[3] in which the debris had about

the same density of 8 pounds per cubic foot but less depth and the debris contained a considerable amount of noncombustible gypsum board instead of all wood. The wind velocity in Experiment 12 was 8 mph compared with 7 mph in Experiment 15. No upwind fire spread rate was measured in Experiment 12 that could be compared with the upwind rate of Experiment 15.

IV MODEL STUDIES OF SIMULATED AIR BLASTS ON STRUCTURES

A. Background

In attempting to study experimentally the combined effects of fire and blast on structures, the major problem is simulating the dynamic effects of blast on the structure. In investigating feasible methods of using full-scale or model structures for blast-fire relevant tests, one suggested way of simulating the blast effects on a building is to enclose a building, possibly with a sheet of plastic, so that a partial vacuum could be created in the building. The vacuum can then be released to simulate air at a higher pressure filling the building, as would occur when a shock wave hits the building. A building collapsed by a shock wave might also be simulated by sufficiently strengthening building support members to withstand the static pressure exerted on the roof and walls as the building was being partially evacuated, and then knocking out the additional supports to collapse the building. If the added supports on the side of the building theoretically facing the blast were withdrawn at the moment the windows were broken to begin the filling process, the building might respond as if it had been hit by a shock wave.

To test the feasibility of using the vacuum air-bag technique to simulate a shock wave on full-scale structures, the technique was tried with a one-tenth scale model of Camp Parks barracks sections.

B. Test Procedures

A scale-model building was patterned after buildings used in the Camp Parks full-scale burn program ex ept there were six rooms in the model, three on each side of a hallway, instead of the normal eight

rooms that the full-scale structures had. A picture of the model is shown in Figure 4(a). The wall and roof joists were made of 1/4- by 1/2-inch strips of particle board and 1/16- by 1-inch strips of balsa wood were used for siding and roofing. These materials were selected because they would break with small loads. The back wall and the back of the roof were made of 3/4-inch-thick particle board to prevent collapse. Siding was omitted from one end so that the interior of the building could be viewed photographically through a plexiglass shield throughout the experiment. The walls and roof of the model were designed and tested so that, with no additional supports, they would fail at pressures in excess of 1 pound per square inch. Additional supports, as shown in Figure 4 (c), that could be knocked out at the appropriate time were added to allow the walls and roof to withstand higher overpressures.

The model building was enclosed in a sheet of 2-mil-thick polyethylene, as shown in Figure 4(b). The air pressure in the interior of the building could be reduced 2 psig below atmospheric pressure with a vacuum pump. A 6-inch length of mild detonating fuse was taped to each window that, when detonated, would break the window and allow air to rush into the building much as the air behind a shock wave from a large yield nuclear detonation would enter a building. A mild detonating fuse was also used to break the additional supports to the walls and roof so that the building would collapse as if no additional supports were present. The mild detonating fuse strung through the supports can be seen in Figure 4(c).

A Kistler pressure gauge connected to an electrical transducer was used to determine the pressure history in the interior of the building from the time the windows were broken until the interior pressure equilibrated with the atmospheric pressure. A motion picture camera that takes pictures at 500 frames per second viewed the interior of the building through the plexiglass shield.

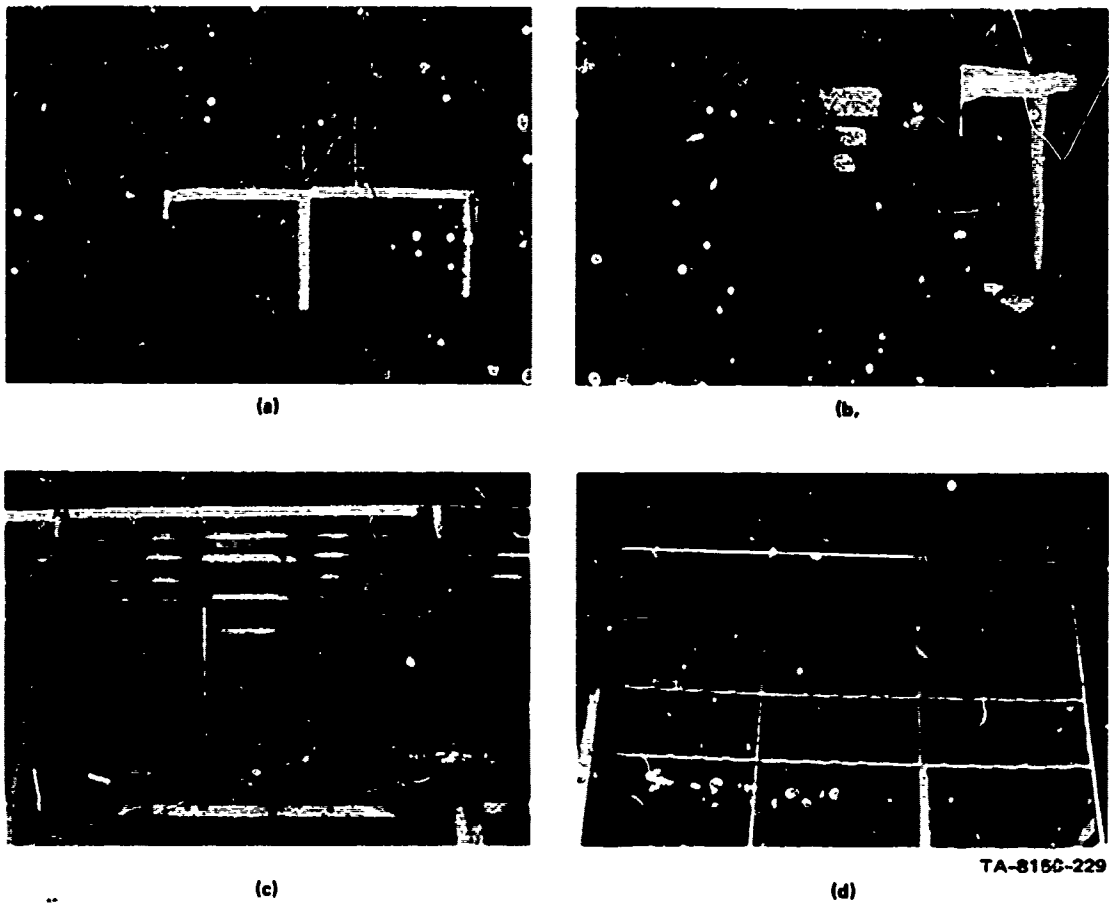

FIGURE 4 PHOTOGRAPHS OF THE SCALE MODEL STRUCTURE USED IN THE AIR BLAST SIMULATION EXPERIMENT

We conducted three tests with the model. For the first test, asbestos paper was glued to the wall and ceiling joists of one of the rooms to enclose the room. Several tissue paper streamers were hung from the ceiling to show the air motion. A curtain was hung on the window and some small furniture simulations were also placed in the room. The pressure in the building was reduced 1 psig, and then the window to the enclosed room was broken while the interior of that room was being viewed photographically.

For the second test the asbestos paper was removed from the walls and ceiling of the one room that had been enclosed in the first test, so that only the room frames remained in the interior of the building. The window that was broken in the first test was replaced. In this test two windows were broken after the interior building pressure had been reduced 1 psig. The air flow and filling process were observed much as in the first test.

In the third test the pressure in the building was reduced 1.8 psig and then two windows were broken at the same time that the additional supports to the walls and roof were broken. The first few times that we attempted to reduce the pressure more than 1.5 psig, weak areas in the structure cracked and holes were punched through the plastic, prematurely and slowly releasing the vacuum. We had planned to reduce the pressure 2 psig before the windows and supports were broken, but the building appeared to be on the verge of collapse when the pressure difference reached 1.8 psig; consequently, we stopped there for the final test.

C. Test Results

In the first test, after the window had been shattered by the mild detonating fuse, pieces of glass could be seen rushing into the room. The motion pictures also showed the window curtain flying across the room, some of the furniture tipping over, and the tissue paper streamers waving.

The modeled room-filling process appeared to be a good visual simulation of real blast effects on structures that do not collapse.

The P ler gauge, with which the continuous pressure and hence the filling time was to be measured, recorde. more noise than signal, and therefore the pressure measurement was unsuccessful. However, we could estimate the filling time for the room from the streamer and glass motion recorded by the motion pictures. Of course, particles with density greater than air will not completely follow the air motion. The forward momentum imparted to the particles during the positive phase of filling will cause the particles to continue in a forward direction during the initial portion of the negative phase. We took this fact into account in estimating the filling time of 15 to 20 msec from the motion pictures.

The time when filling is complete, τ, has been estimated to be:[9]

$$\tau = 0.422 \frac{V_r}{A_w} \sqrt{\Delta P_o} \text{ milliseconds,}$$

where

V_r is the volume of the room being filled in cubic feet

A_w is the area of the window opening in square feet

ΔP_o is the initial difference in pressure of the interior and the exterior of the building

If the room enclosed in asbestos paper with a volume of 1.7 cubic feet is used as the volume being filled, the filling time for $A_w = 0.14$ square feet and $\Delta P_o = 1.0$ psi is estimated to be 5.1 msec. If the total volume of the building of 18.7 cubic feet is used, the filling time is 56 msec.

The measured filling time of 15 to 20 msec is between the calculated value for filling only the room and filling the entire building. This is not too surprising since there were many paths for the air to leak from

the enclosed room to the rest of the interior, yet the room would appear filled before the entire building equilibrated with the room.

In the second test in which two windows were broken and the building interior was entirely open, the filling time estimated from the motion picture is 20 to 25 msec. In this case in which A_w = 0.28 square feet V_r = 18.7 cubic feet, and ΔP_o = 1.0 psi, the calculated filling time is 28 msec, which compares favorably with the measured time. Again the Kistler gauge failed to record the pressure satisfactorily.

In the third and final test with the model in which the additional supports as well as two windows were broken when the pressure was reduced 1.8 psi, several long but narrow cracks developed in the siding and roofing and a few of the building joists were broken, but the building did not fail catastrophically as expected. Figure 4(d) shows the building after the third test; the additional supports are broken but the rest of the building has only minor damage. The net force on the exterior of the building was relieved before the building collapsed. The building did not respond as we had hoped because it did not respond as a building would to the blast wave of a nuclear detonation of corresponding peak overpressure.

D. Conclusions

The model experiments show that it would be difficult to use the Camp Parks barracks buildings in blast-fire experiments as we had planned, that is, we could not simulate the effects of a blast wave hitting a building by creating a partial vacuum inside a building and suddenly releasing that vacuum. The problem of a weak structural portion of the building prematurely breaking and slowly releasing the vacuum would be compounded in scaling from the scale model to a large building. For the partial vacuum method of collapsing a building to simulate accurately the effects of the blast of a nuclear weapon, the building would have to be uniformly stressed

almost to the point of collapse before the additional strengthening members are removed. Such a condition would be difficult to attain because weak points in the structure would be almost impossible to eliminate.

However, the model experiment did show another experiment for which the partial vacuum method would be useful. The effects could be studied of a shock wave entering and filling a room in which the window was broken but the structure did not collapse. The method would well simulate the effects of such a shock wave. From the scaling laws developed in Appendix B, it is now possible to devise reliable models for the investigation of blast-fire interactions during the fluid-flow and fuel redistribution processes accompanying room filling. Such models deserve further research attention.

V THE DYNAMIC EFFECTS OF THE PASSAGE OF AN AIR SHOCK OVER IGNITED MATERIALS

A. Background

For a considerable period of time the fire-research community has recognized and documented the potentially important interactive effects of blast and fire, effects that include both the dynamic influences (enhancement and extinguishment) of the passage of the air shock over ignited materials and the perturbations in fire growth and spread caused by the residual disarray in the target that is produced by blast. The Defense Nuclear Agency (DNA), in two separate documents dealing with the wild land environment[17,18] published under the auspices of The Technical Cooperation Program (TCP), acknowledges that fire effects are potentially serious results of the tactical use of nuclear weapons in the forests and stresses the uncertainties in fire-damage evaluation attendant on the as yet inadequately evaluated interactions with blast effects. In more recent events, DCPA has recognized the potential importance of blast-fire interactions in the evaluation of urban damage and the associated necessity for planning of civil defense countermeasures and emergency operations. Without risk of exaggeration, it can be said that the fire problem following nuclear attack swings from manageable to unmanageable on the credibility of the assumptions that can be, and are being, made concerning the dynamic and residual influences of air blast and its effects on the incendiary responses of combustible target elements.

The few combined blast-fire experiments that have been conducted to date in urban target simulations[11] suggest that the principal dynamic effect of the passage of the blast wave is the extinction of flaming combustion in interior fuels at free-field overpressures in the range of 2 to 3

psi, and that the result is not sensitive to either the kinds of fuels or the relative sizes of the wall openings through which the external blast-induced environment propagates its effects on the interior of a structure. It may be the pressure discontinuity, then, rather than the flow field, that is responsible for flame extinguishment. Further confirmation of this conclusion is currently being sought.

In these same tests, high-speed motion pictures reveal that flames are swept from the burning fuel item in an apparent shearless displacement of the air above the burning surface. This displacement causes the complete removal of the flames from the fuel without the development of a boundary layer that would, under more usual circumstances (e.g , in the flow field of a high speed wind tunnel), reestablish the combustion process following the disturbance.

It is worth noting that a mechanism of blowout, such as the postulated shearless displacement, is not applicable without limit to large fuel items. It is well known, for example, that boundary layer flow does develop a short time after the diffraction of a shock wave across an object. If the object is sufficiently large in the direction of propagation, this boundary layer may appear before the flame has been totally displaced beyond its downstream edge. In such a case, flaming combustion may readily reestablish itself. Given this possibility, we attempted to ascertain the limiting size of objects for which extinguishment is not possible and how this limiting size varies with the characteristics of the incident shock. Our experiment was done at the Mixed Company Event, which was a 500-ton TNT blast and shock experiment designed to provide experimental data for the solution of nuclear weapon problems.

B. Experimental Plan

Our experiment consisted of a series of burning fuel plots of varying dimensions designed to establish the empirical dependence of fire size

(i.e., flame displacement) on the peak overpressure/positive-phase duration of the blast wave that is just capable of extinguishment. The basic measurement consisted of determining through photographic observation the smallest plot size that will just sustain flaming combustion throughout the dynamic disturbance resulting from the passage of the blast wave.

The theoretical basis for the experimental design was derived from the boundary-layer mechanics of nonsteady fluid flow and the principle of "critical flame stretch" advanced by Karlovitch.[19] It is postulated that, for a given set of conditions, the transition from nonsteady to steady flame is dependent only on the local velocity gradient normal to the surface supplying the volatile fuel. Thus the passage of the shock gives momentary rise to a discontinuous (i.e., infinitely steep) gradient at an air-solid interface, through which a steady flame cannot maintain itself. Following the passage of the shock, this discontinuous gradient is replaced with a steep velocity gradient that becomes shallower with time until, at some later time and at a point downstream of the first encounter between the fire and the shock if fuel and flame are still adjacent to one another, the flame speed is at last sufficient to hold a steady flame against the flow field. Obviously this will occur at a point in time before the free stream velocity has fallen to zero, and therefore the flames will have displaced a distance rather less than the particle displacement that accompanies the passage of the shock. How much less will depend on an unknown number of factors, but these will surely include the roughness of the air-solid interface and will probably include, as an important factor, the peak overpressure of the blast wave. For a moderately smooth surface fuel bed, we expected that the extent of the flame displacement, relative to the particle displacement, would be directly proportional to the free stream velocity and inversely proportional to the square root of the positive-phase duration.

Fuel plots were constructed at three stations, one station 1,400 feet south of ground zero, the second station 2,400 feet south of ground zero, and the third station 4,000 feet south of ground zero (see Figure 5). The predicted air blast parameters at these three locations are given in Table 1. The measured peak static overpressures were slightly greater than those predicted and the measured durations of positive overpressure were very close to the predicted durations. However, the differences between the measured and predicted air blast parameters are not significant to the results of our experiment.

At Station 1, 6 fuel plots were constructed that were 3.5 feet wide and 5, 9.5, 19, 24, 28.5, and 38 feet long in the direction of shock propagation; these lengths ranged between 0.14 and 1.12 x_p, where x_p is the predicted particle displacement in a free field due to the passage of the shock wave. We hoped that the range of pan sizes would permit at least one fire to be extinguished and at least one fire to survive the passage of the shock wave. The fuel plots were galvanized steel pans 3 inches deep filled with 1/2- to 1-inch-diameter rocks. The largest pans were 3.5 by 9.5 feet; therefore the larger fuel plots required several pans butted together. The pans were filled with water to 1/8-inch from the top edge. One-eighth inch of kerosene was floated on the water; therefore the kerosene reached the lip of the pans. The top edges of the rocks were below the kerosene surface. Dirt and rocks were graded to the outside edges of the pans so that the top edges of the pans were at ground level and the pans did not present a sharp edge to the shock wave to disturb the air flow.

Fuel plots at Stations 2 and 3 were similar to those at Station 1 except that they were shorter in length. At Station 2 seven fuel plots had dimensions in the direction of shock propagation of 1, 3, 4, 5, 6, 8, and 19 feet, and at Station 3 seven fuel plots had lengths of 0.5, 1, 2, 3, 4, 6, and 12 feet.

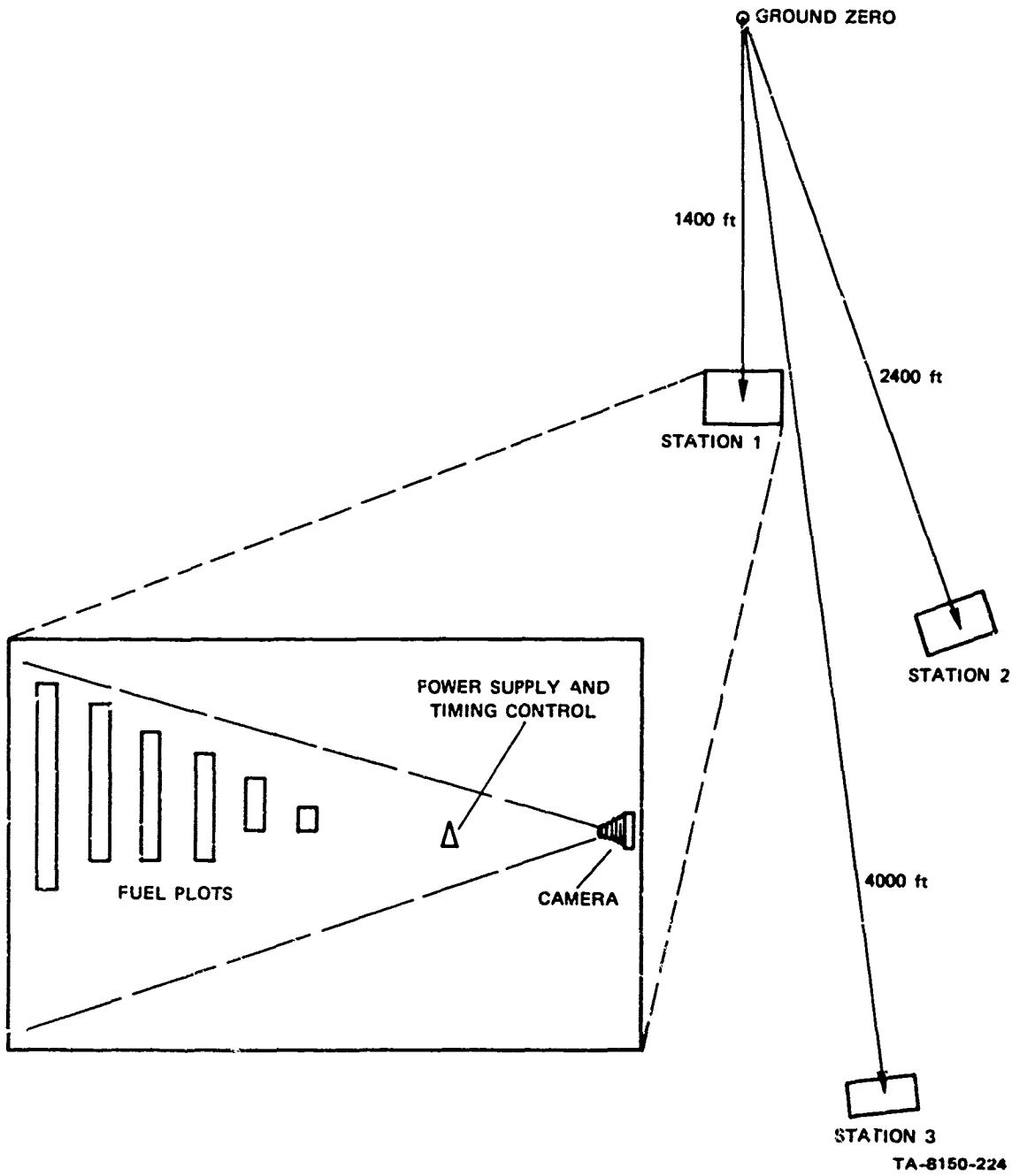

FIGURE 5 SITE PLOT PLAN FOR FLAME EXTINGUISHMENT EXPERIMENT

Table 1

PREDICTED AIR BLAST PARAMETERS AT THREE LOCATIONS

	R (ft)	ΔP (psi)	t^+ (msec)	U (ft/sec)	u_o (ft/sec)	x_p (ft)
Station 1	1400	5	315	1304	294.3	34.1
Station 2	2400	2	395	1193	128.7	18.7
Station 3	4000	1	460	1154	66.5	11.3

R = ground range or distance from ground zero

ΔP = peak static overpressure

t^+ = duration of positive overpressure

U = shock front velocity

u_o = peak particle velocity in a free field

x_p = particle displacement in a free field

ΔP and t^+ = predicted values taken from the Middle North Series Mixed Company Event Technical and Administrative Document

$$U = c_o \left(1 + \frac{6\Delta P}{7P_o}\right)$$

$$u_o = \frac{5\Delta P}{7P_o} \frac{c_o^2}{U}$$

$$x_p = u_o t^+ e^{-1}$$

where

P_o = ambient pressure, estimated to be 11.53 psi

c_o = speed of sound in air, estimated to be 1113 ft/sec .

The fires were ignited by an electric squib, Hercules S26BO, to which four wooden matches were taped and to which was connected a plastic bag filled with approximately two quarts of gasoline. Several ignit rs (squib, matches, and gasoline) were placed on each fuel plot to ensure ignition of the entire plot area. A timing signal 2 minutes before the blast closed a circuit between the electric squib and a 12-volt wet cell. The squib then ignited the matches, which in turn melted the plastic bag and ignited the gasoline. The flaming gasoline then spread over the kerosene and ignited the entire fuel plot. The fires reached full intensity in 2 minutes. There was sufficient kerosene for the fuel plots to burn for more than 3 minutes at full intensity.

The fires of each of the three stations were photographed by an 8-mm movie camera running at 24 frames per second. In addition, a 16-mm movie camera was used at Station 1. A timing signal started the cameras 15 seconds before the blast. The fuel plots and their identification markers were located so that the fires on the six or seven fuel plots at each station were easily distinguishable on the films.

C. Results

No fire at any of the three stations was extinguished by the shock wave.

At Stations 2 and 3 all the fuel plots were fully ignited by the time of the blast and the cameras operated as designed throughout the test. The flames were stretched by the shock and following airflow, but they remained in contact with the fuel plot. The flames appeared to maintain contact even with the front edge of the fuel plots. The top edge of the flames formed a profile typical of a boundary layer beginning at the front edge of the pan.

At Station 1 the signals to both cameras were interrupted by the blast, and we obtained only one frame of pictures after the shock wave reached the fuel plots. The one frame of pictures shows that the flames were maintaining complete contact with the fuel plots. From our observation point on a bluff approximately three miles away, we could see no decrease in flames caused by the shock wave, indicating that no fires were extinguished; however, individual plots could not be distinguished. We could not reignite fire on any of the fuel plots when we reentered the area, which is further evidence that all the fuel was burned and that none of the fires was extinguished.

The weather at the time of the test was clear, with a temperature of about 40°F and a ground wind of 2 or 3 mph in a direction from our stations toward ground zero. The ground was covered with about an inch of snow that the shock wave appeared to kick up as it moved, but this snow did not affect the fires.

D. Conclusions

The shock wave apparently did not create a shearless displacement of the flames from the fuel in our experiment--as was postulated to occur. A boundary layer appeared to form at the front edge of the fire, thereby holding the flames in contact with the fuel. This result seemingly contradicts the conclusion of a previous experiment[11] in which a shock wave swept the flames from the fuel in an apparent shearless displacement, thereby separating the flames from the fuel and extinguishing flaming combustion. It may be that the effect of passage of a shock wave over a fire is sensitive to the kind of fuel; our fuel was a liquid rather than the solid fuel used in the previous experiment. Or a boundary layer may have formed above our fuel plots because the fuel had burned slightly below the lip of the pan by the time of the blast; however, this is not a likely explanation for the lack of extinguishment of our fires.

It was pointed out at the Mixed Company Results Meeting[20] that the shock front was degraded near the ground and that the fuel plot surfaces that were flush with ground may not have experienced free-field overpressures. It was also thought that the shock discontinuity might be degraded to potential flow near the surface. Had our fuel plot surfaces been elevated several feet above the ground, the shock wave might have had an entirely different effect on the flames.

The mechanism of flame extinguishment by a shock wave needs to be further investigated so that one can predict which kinds of fires will be extinguished by the blast wave in the event of a nuclear detonation. One experiment[11] postulated that most flaming combustion would be extinguished by a shock wave with a free-field overpressure greater than 2 or 3 psi. But in our experiment, not even a 5 psi, free-field overpressure shock wave extinguished any fires. It is therefore obvious that more information is needed on the mechanism of flame extinguishment by a shock wave and the dependence of flame extinguishment on the physical characteristics of the fire and its surroundings.

REFERENCES

1. C. P. Butler, "Measurements of the Dynamics of Structural Fires," OCD Work Unit 2561A, Annual Report, Project PYU-8150, Stanford Research Institute, Menlo Park, California (August 1970).

2. S. J. Wiersma and S. B. Martin, "Measurements of the Dynamics of Structural Fires," OCD Work Unit 2561A, Annual Report, Project PYU 8150, Stanford Research Institute, Menlo Park, California (August 1971).

3. S. J. Wiersma, "Measurements of the Dynamics of Structural Fires," DCPA Work Unit 2561A, Annual Report, Project PYU 8150, Stanford Research Institute, Menlo Park, California (August 1972).

4. C. K. Wiehle and J. L. Bockholt, "Existing Structures Evaluation, Part V: Applications," OCD Work Unit 1154F, Final Report, Project 6300, Stanford Research Institute, Menlo Park, California (July 1971).

5. C K. Wiehle and J. L. Bockholt, "Blast Response of Five NFSS Buildings," OCD Work Unit 1154I, Technical Report, Project 1219, Stanford Research Institute, Menlo Park, California (October 1971).

6. J. Rotz, J. Edmunds, and K. Kaplan, "Formation of Debris from Buildings and their Contents by Blast and Fire Effects of Nuclear Weapons," URS Research Corporation Report, Burlingame, California (January 1966).

7. A. Longinow and G. Ojdrovich, "Survival Prediction Analysis," IIT Research Institute, Chicago, Illinois, (November 1972).

8. A. Longinow and G. Ojdrovich, "Computer Program for Predicting the Safety of People in a Direct Effects Nuclear Weapon Environment," IIT Research Institute, Chicago, Illinois.

9. S. B. Martin, R. W. Ramstad, T. Goodale, and C. A. Start, "Effects of Air Blast on Urban Fire Response," OCD Work Unit 2534F, Final Report, URS Research Corporation, Burlingame, California (May 1969).

10. J. McAuliffe and K. Moll, "Secondary Ignitions in Nuclear Attack," OCD Work Unit 2534 A, Stanford Research Institute, Menlo Park, California (July 1965).

11. T. Goodale, "Effects of Air Blast on Urban Fires," OCD Work Unit 2534I, Final Report, URS Research Corporation, Burlingame, California (December 1970).

12. C. K. Wiehle, "All-Effects Shelter Survey System--Summary of Dynamic Analysis of 25 NFSS Buildings," Technical Report for DCPA, Stanford Research Institute, Menlo Park, California (March 1973)

13. A. Longinow, G. Ojdrovich, L. Bertram, and A. Wiedermann, "People Survivability in a Direct Effects Environment and Related Topics," DCPA Work Unit 1614D, Final Report, IIT Research Institute, Chicago, Illinois (May 1973).

14. Environmental Science and Technology, Vol 5, No. 3, p. 213 (March 1971).

15. C. H. Yuill, Fire Journal, Vol. 66, No. 3 p. 47 (May 1972).

16. Private Communication with T. E. Waterman, IIT Research Institute, Chicago, Illinois.

17. J. J. Meszaros, and J. R. Kelso, eds., "Nuclear Weapons Effects in a Forest Environment-Blowdown (U)," N2:TR 1-69, Published by G. E. Tempo, Santa Barbara, California (August 1969), CONFIDENTIAL.

18. J. W. Kerr et al., "Nuclear Weapons Effects in a Forest Environment--Thermal and Fire (U)," G. E. Tempo (DASIAC), Santa Barbara, California (July 1971), UNCLASSIFIED.

19. B. Karlovitch, "Flame Stabilization in Fast Streams," Sixth Symposium on Combustion of the Combustion Institute, p. 941, (Reinhold Publishing Corporation, N. Y., 1956).

20. Discussion at the Mixed Company Results Meeting, Santa Barbara, California, March 13-15, 1973.

Appendix A

AN URBAN MODEL FOR EVALUATING COMBINED EFFECTS OF BLAST AND FIRE

By

Stanley B. Martin

Appendix A

AN URBAN MODEL FOR EVALUATING COMBINED EFFECTS OF BLAST AND FIRE

The surest way to test one's ability to predict, describe, and assess the combined damaging effects of a catastrophic disaster, such as nuclear attack, and at the same time to discover just what one cannot do without resorting to outright guesswork, is to attempt a detailed description of the disaster on a real city. The task is rarely attempted in earnest because it is an overwhelmingly enormous one. Still, it is the ultimate proof of the accomplished art, short of testing the prediction by reproducing the disaster experimentally.

A satisfactory substitute for a real city is a hypothetical one. In fact, a hypothetical city can be designed to improve on real cities whenever the results of the analysis to be performed on the city are to be interpreted as generally applicable to all similar urban situations. Even more to the point in the present case, a hypothetical city can be synthesized from component structures about which considerable detailed knowledge already exists both to ease the work required in doing damage assessment and to achieve a high expectation of confidence in the results.

The hypothetical urban area used in the present study was designed with these factors in mind. In particular, the buildings chosen to make up the area were selected from a population of buildings that had already received substantial attention to ascertain their blast vulnerability, it being assumed that this would allow us to describe readily and confidently their response to various damaging levels of blast overpressure.

An added benefit was expected to be derived from the rather detailed information that had been collected about these buildings from plans and on-site inspection--details that would be required for estimating fire responses as well as blast effects.

The hypothetical urban area is depicted in Figure A-1. All of the foreground buildings are actual buildings in various U.S. cities that have been grouped together in a reasonable simulation of a downtown area of a moderately large city. Figure A-2 is a plan view of the area. Care has been used to retain contiguous building arrangements wherever they existed in the real situations.

The individual buildings are identified in Table A-1. The first five are NFSS structures located in the Greensboro-High Point SMSA of North Carolina. Blast response analyses of these buildings are reported in Ref. 1, which contains a description of the buildings and lists relevant details about them. The remaining ten buildings were selected from the 25 NFSS buildings that were recently surveyed by Research Triangle Institute as a part of an all-effects shelter analysis.[2] The blast analysis of these buildings was performed by SRI, and details are summarized in Ref. 3.

For purposes of synthesizing the hypothetical urban area, a few minor liberties were taken. The RCA building was lowered to 30 stories so that it would not seem out of place in relation to the other buildings. Building 62A was made to resemble a major hotel by putting together sections equivalent in size and construction to Building 62. These changes are not expected to alter the basic blast-response vulnerability of these buildings, however.

In conducting the analysis, we decided to settle on a particular weapon yield (5 MT) and to place the explosion ground zero at varying

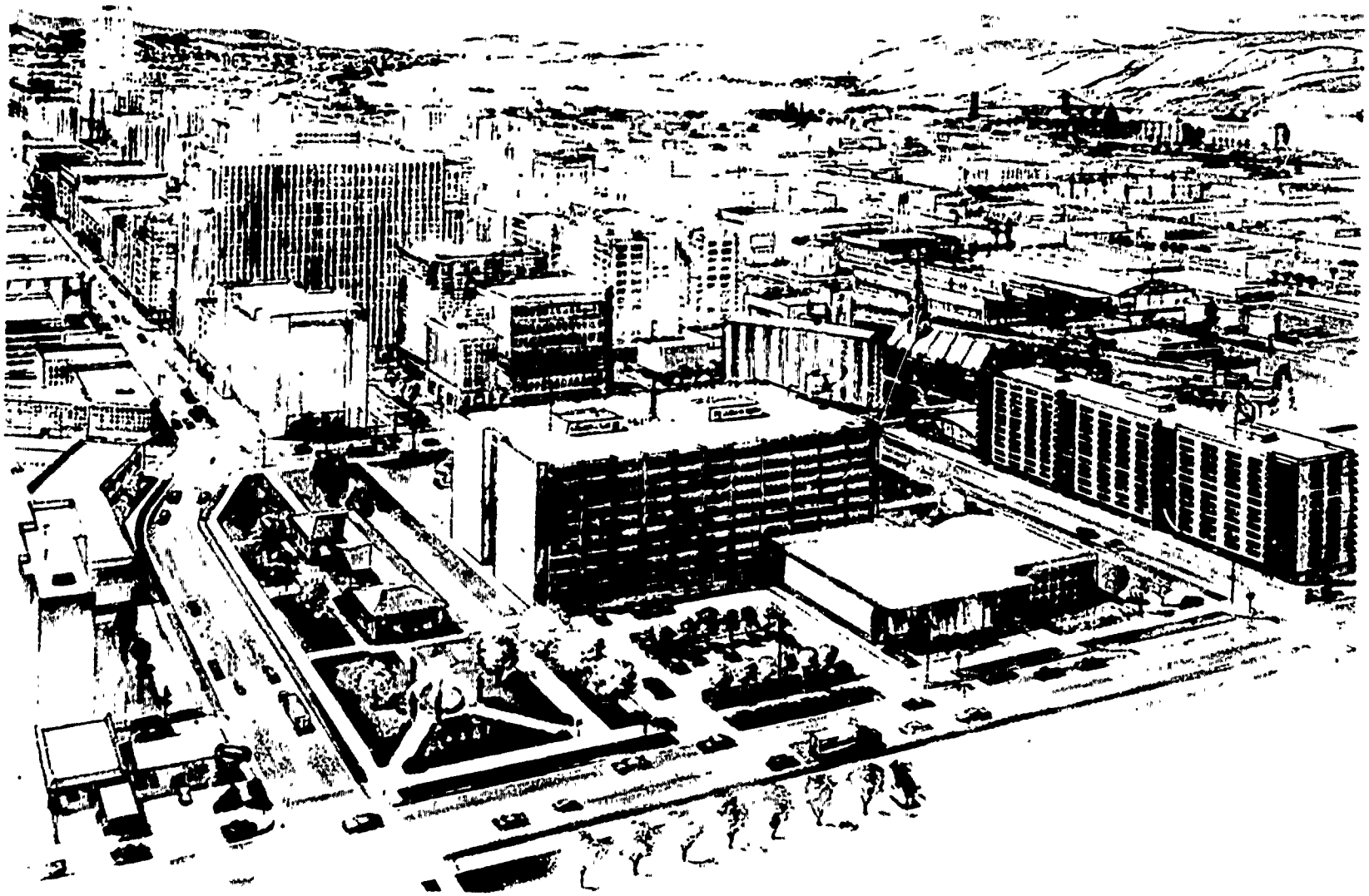

TA-8150-260

FIGURE A-1 HYPOTHETICAL URBAN AREA

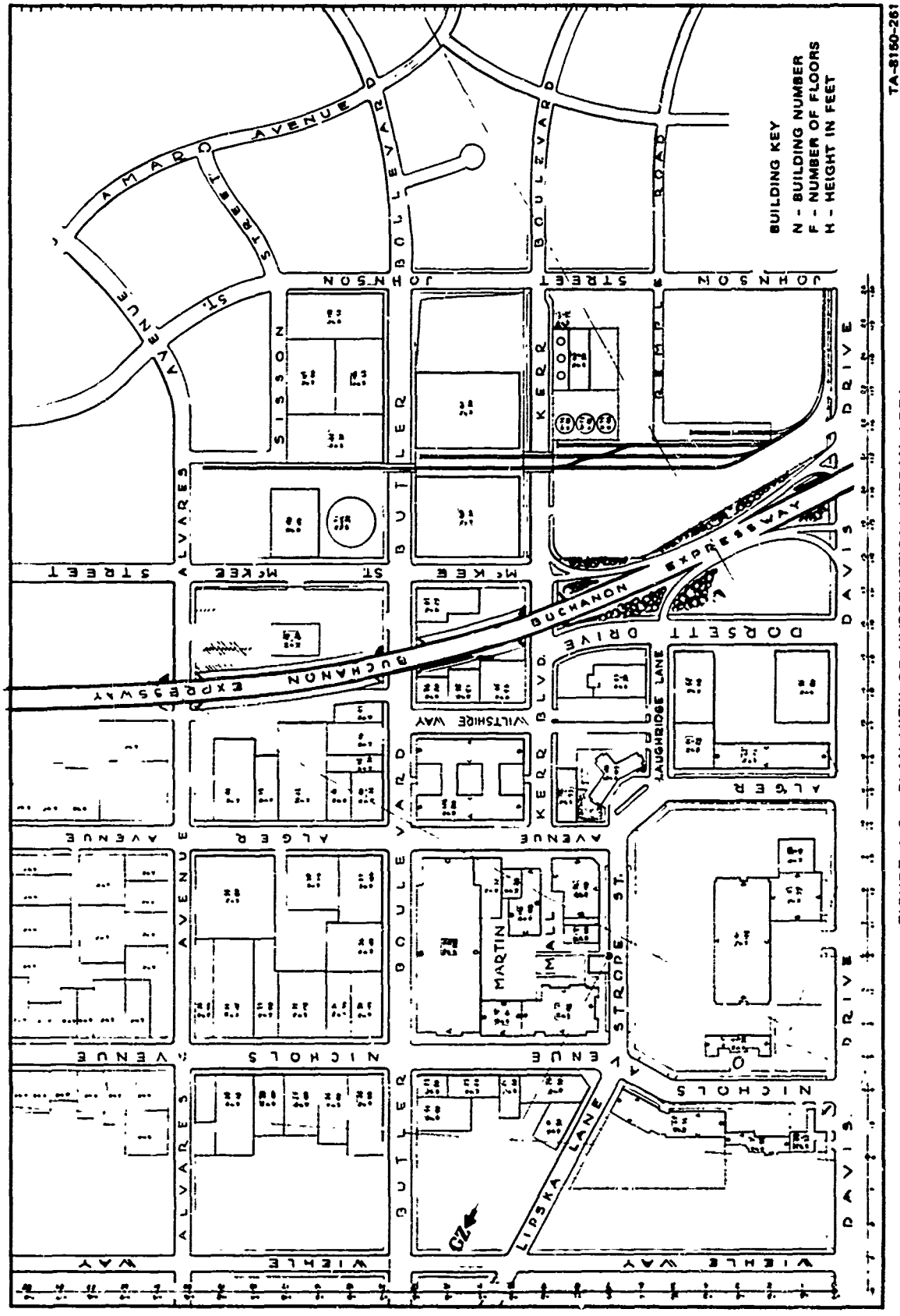

FIGURE A-2 PLAN VIEW OF HYPOTHETICAL URBAN AREA

Table A-1

BUILDINGS SELECTED FOR ANALYSIS

Building No.	
1	Southern Furniture Exposition, Greensboro, N. C.
2	Public Library, Greensboro, N. C.
3	Laura Cone Dormitory, Greensboro, N. C.
4	Willa B. Player Hall, Greensboro, N. C.
5	North Carolina National Bank, Greensboro, N. C.
13	Leavitts Store, Manchester, N. H.
51	RCA Building (shortened to 300-ft height), New York, N. Y.
62	Atlantis Apartments, Rockaway Beach, N. Y.
62A	Atlantis Apartments (enlarged)
63	Junior High School, Amityville, N. Y.
76	Garfinkel's Department Store, Washington, D. C.
81	Federal Office Building, Louisville, Ky.
136	First Federal Savings and Loan, Augusta, Ga.
140	Sunrise Towers, Winston-Salem, N. C.
146	Marine Drive Apartments, Chicago, Ill.

distances from the test area, along a fixed azimuth, to provide several example peak overpressures in the 1- to 10-psi range. The values initially selected were 2, 3, 5, and 10 psi. Differences between surface and low air bursts were also noted. Apparent fireball sizes viewed at distances corresponding to these overpressures are illustrated in Figure A-3. Estimates of thermal radiation exposures are given in Table A-2.

Once the burst point was selected, it was then possible to lay out the areas of thermal shielding on the target, as illustrated in Figure A-4, and in so doing to prescribe which buildings and portions of buildings were exposed and even the number and location of windows exposed to the thermal pulse in any given floor of a particular building. This allowed estimates of fire starts to be made (See Appendix D).

Blast damage was evaluated by noting whether the incident overpressure exceeded the published values for the incipient collapse overpressure of exterior walls and by how much. Figure A-5 illustrates the somewhat subjective estimate of the appearance of one of the buildings (whose exterior walls had been predicted to fail incipiently when loaded at normal incidence with a 1 1/2-psi peak overpressure shock wave) after being subjected to only 2 psi overpressure. Using a set of drawings like the one shown in Figure A-5 to illustrate the damage to each building in the area when it experiences progressively increasing overpressures, one could achieve a composite picture of the damage to the city area. Then using the results of the debris model, one could illustrate the nature and extent of the debris distributed over the streets and open spaces between buildings.

The intention of the work started here was to complete an illustrated description of the attack environment as outlined above. Unfortunately,

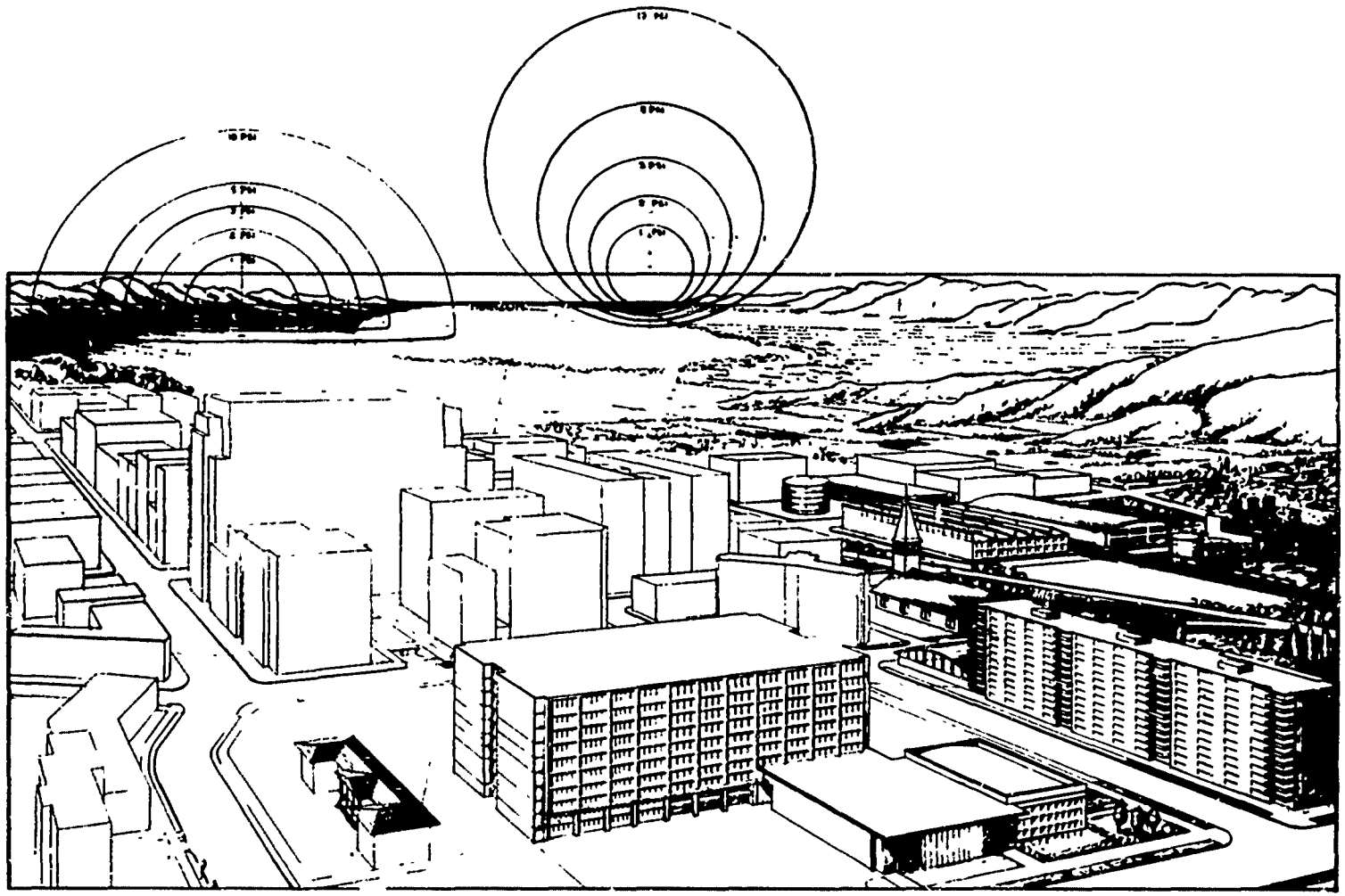

TA-8150-262

FIGURE A-5 FIREBALL SIZE AS VIEWED AT DISTANCES CORRESPONDING TO 1, 2, 3, 5 AND 10-psi PEAK OVERPRESSURES

Table A-2

THERMAL RADIATION EXPOSURES (cal cm^{-2})
AT DISTANCES CORRESPONDING TO VARIOUS
AIR BLAST PEAK OVERPRESSURES
(5-MT Explosion; 10-Mile Visibility)

Burst Type	Peak ΔP (psi)	Distance (mi)	Elevation Angle* (deg)		Radiant Exposures (cal cm^{-2}) β = 0	Radiant Exposures (cal cm^{-2}) β = 5°
Surface burst	1	12.5	4.0		4.5	0
	2	8.0	6.3		20.7	2.2
	3	6.3	7.9		41.9	10.8
	5	4.7	10.5		90.1	38.2
	10	3.26	15.1		221	131
Airburst						
1 fireball			0†	5.4†		
radius height	1	14.8	0		3.8	0
of burst (HOB)	2	9.1	0	8.8	22.7	10
	3	7.1	0	11.4	49.7	26
	5	5.2	0	15.7	114	70
	10	3.55	0	22.8	290	280
2 fireball						
radii HOB			2.4†	7.1†		
	1	17.0			2.0	1.0
	2	10.2	4.0	11.8	15.1	14.0
	3	7.8	5.2	15.5	35.4	35.4
	5	5.7	7.2	21	84.2	84.2
	10	3.8	11.0	32	215	215

*Line of sight to top of fireball
†Lines of sight to top and bottom of fireball(s).

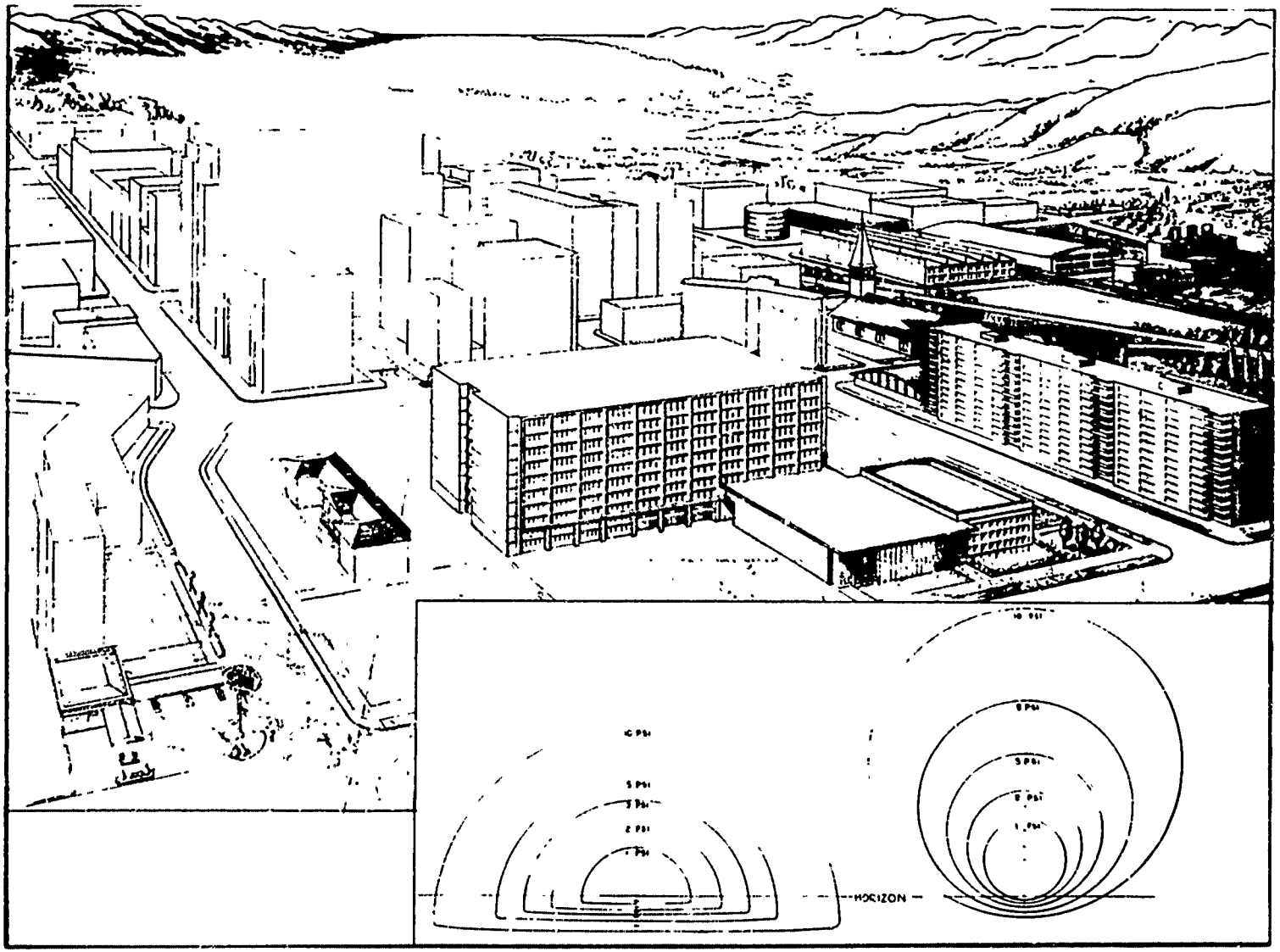

TA-8150-263

FIGURE A-4 THERMAL SHIELDING ON THE TARGET

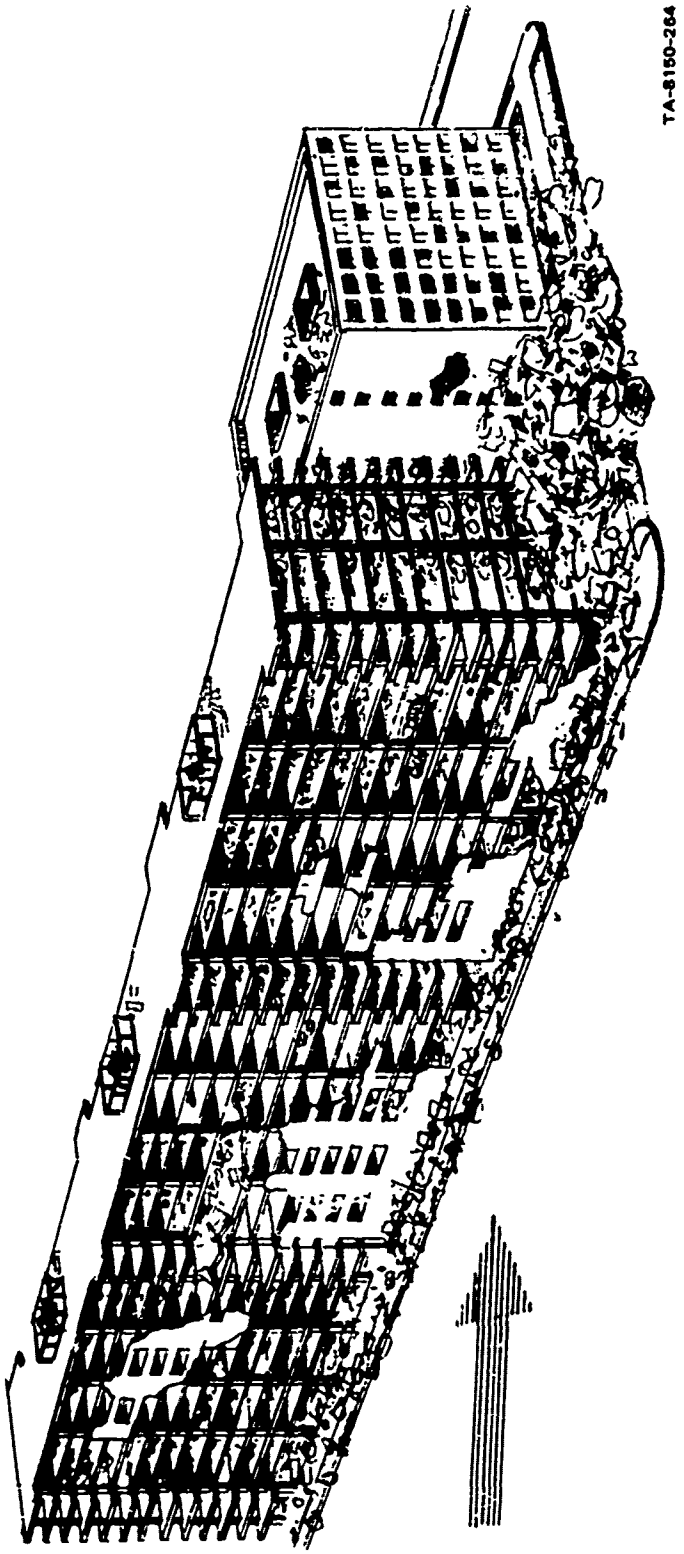

TA-8150-264

FIGURE A-5 BUILDING 62 FOLLOWING A 1½-psi PEAK OVERPRESSURE SHOCK WAVE

as already noted in the body of this report, the present state of the art does not provide a sufficient technical basis for accomplishing such a description. Although the threshold overpressures for wall collapse have been calculated for these buildings, the results of these calculations do not allow useful extrapolations of damaged states to be drawn for overpressures that appreciably exceed the threshold values. This limitation also seriously hampers our ability to treat the description of debris formation, translation, and final distribution. An analytical approach to guide the making of the necessary extrapolations is described in the Appendix B.

REFERENCES

1. C. K. Wiehle and J. L. Bockholt, "Blast Response of Five NFSS Buildings," OCD Work Unit 1154 I, Technical Report, Project 1219, Stanford Research Institute, Menlo Park, California, (October 1971).

2. C. K. Wiehle, "All-Effects Shelter Survey System--Summary of Dynamic Analysis of 25 NFSS Buildings," Technical Report for DCPA, Stanford Research Institute, Menlo Park, California, (March 1973).

3. D. F. Tolman, R. O. Lyday, and G. M. Botkin, "Estimated Characteristics of NFSS Inventory," Technical Report for DCPA, Research Triangle Institute, Research Triangle Park, North Carolina, (November 1972).

Appendix B

MODELING STRUCTURAL RESPONSES TO AIR BLAST LOADING

By

A. Murty Kanury

Appendix B

MODELING STRUCTURAL RESPONSES TO AIR BLAST LOADING

Our attempts to develop techniques of experimentally modeling the blast/fire phenomenon culminated in delineation of the problem into two separate parts: Problem 1, the blast/structure interaction and Problem 2, blast/(collapsed) structure/fire interaction. The results of Problem 1 are expected to be input conditions for Problem 2.

Literature contains some information relevant to Problem 1 and practically no information on Problem 2. Notable contribution to Problem 1 is made by Wiehle and Bockholt[1] under the sponsorship of DCPA to develop an all-effects shelter survey system that evaluates the response of existing structures when subjected to air-blast loading.

Development of an experimental modeling technique requires formulation of the problem with the essential mechanistic details to arrive at the nondimensional variables that are ratios of the quantities exerting control over the behavior of the system and that therefore must be kept invariant between the model and prototype. Since the study objectives of Wiehle and Bockholt do not directly invoke deduction of these modeling laws, we have undertaken the analyses that follow.

Our goal is to develop scaling laws relating a small-scale modeling experiment with a life-size prototype system that facilitates study of the blast/structure interaction phenomenon. Development of scaling laws always entails minimization of variables in the problem by dimensional analysis and establishment of functional forms of the solutions. Specifically, the questions asked include: What is the time history of net pressure across the windowed wall of a chamber following the incidence

of a blast wave? How long does it take to fill the room and hence to nullify the net loading on the wall? What sort of a flow pattern is expectable in the chamber before collapse? How does the threshold overpressure causing collapse depend on the room, window, and wall properties? For higher overpressures, how do the time, velocity, and acceleration of collapse depend on the properties of the system? These and other related questions are to be answered with a set of consistent non-dimensional variables enabling scalable general predictions.

1. The Room Filling Process

Following Melichar's[2] work and Shapiro's[3] text on compressible flow, consideration of the mass and energy conservation for "steady" isentropic flow through a sharp-edged window orifice of area A in the wall (of area A_w, density ρ_w and thickness T_w) of a chamber of volume V_c, the chamber pressure P_c variation with time t is given by:

$$\frac{dP_c}{dt} = \frac{A}{V_c} f \quad , \tag{B-1}$$

where f is a function dominantly of the pressure difference across the wall ($P_e - P_c$) and weakly (but highly nonlinearly) of γ, R, $T_{initial}$, and peak overpressure. Experience indicates[4] that f may be approximated (for air at about 25°C with overpressures not exceeding 150 psi) by

$$f = \Delta \, (P_e - P_c)^{1/2} \quad .$$

(Δ is approximately equal to 6700-ft $psi^{1/2}$ sec^{-1}.) Substituting this approximation in Eq. (B-1) and approximating the blast pressure decay by

$$(P_e - P_o) \approx (P_{so} - P_o)\ (1 - t/t_+) \quad ,$$

where $(P_{so} - P_o)$ is the peak overpressure and t_+ is the time of positive pressure phase duration, the problem at hand is:

$$\frac{d\pi}{d\tau} = -\left[\frac{1}{\tau_+} + 2\pi^{1/2}\right] \quad . \tag{B-2}$$

$$\pi\ (0) = 1 \quad ,$$

where the scaled variables are defined as:

$$\pi \equiv \frac{P_e - P_c}{P_{so} - P_o} \quad \text{and} \quad \tau \equiv \frac{t}{\frac{2V_c}{A\ell}\ (P_{so} - P_o)^{1/2}}$$

The solution of Eq. (B-2) is straightforward. It may be simplified, by noting from experience that $1/\tau_+$ is negligible, to

$$\pi \approx (1 - \tau)^2 \quad . \tag{B-3}$$

The most important implications of Eq. (B-3) are two-fold: (1) the load on the wall due to the blast wave varies quadratically with time, and (2) the time to equilibrate the external and chamber pressures (i.e., to fill the chamber) is given by:

$$\tau_f \approx 1 \quad . \tag{B-4}$$

This result is in concurrence with a multitude of experimental measurements, empirical rules, and computer calculations available in literature. In physical terms, Eq. (B-4) indicates that the time of filling t_f is

$$t_f \approx \frac{2V_c}{A\Delta} (P_{so} - P_o)^{1/2} \quad .$$

Consideration of the flow as incompressible also yields the same result as above, provided that the definition of Δ is altered in a minor fashion by a numerical coefficient.

2. Flow in the Room

As the flow emerges into the room through the window at a velocity dependent on the time-variant pressure differential, a well-defined jet may or may not be formed according to whether the ratio of room depth to the length of the jet's potential core is greater or less than unity. From considerations of the mixing flow and the jet diffusion constants available in Schlicting's[5] book on boundary layers, a jet is ensured if the room depth D is greater than $6.25A^{1/2}$. In buildings like some older factories and assembly plants and some modern residential structures, the windows are usually so large that a jet is not fully developed, and the shock traverses clear across the room to reflect off the internal wall. The blast effects on the internal wall consequently become of primary interest. In those architectural styles where the windows are relatively small, a well-defined jet and consequent recirculation flow are formed; the blast effects on interior walls are of secondary interest. The drag effects and resultant translational displacement of the room contents are, of course, drastically different in the two limiting cases discussed above.

We will not deal with the jet formation modeling in detail here because it is composed of an entirely separate, larger problem of fluid dynamics involving submerged bodies. Suffice it to say that the reference velocity is

$$C_d \left[\frac{2g}{\rho} (P_{so} - P_o)^{1/2}\right] \quad ,$$

reference pressure differential is $(P_{so} - P_o)$, reference time is

$$2V_c\left(P_{so} - P_o\right)^{1/2}/A\Delta \quad ,$$

and reference length is $A^{1/2}$.

3. Collapse Dynamics

The response of a windowed wall on which the blast loading is exerted is described by the equation of motion, which expresses the balance between the applied (time variant) load, inertia of deflection, and elastic strain.

$$(A_w - A)(P_e - P_c) = (A_w - A)\frac{T_w \rho_w}{g}\ddot{y} + A_w q(y) \qquad \text{(B-5)}$$

The distributed loading, deflection, and resistance functions are, in real situations, very complicated functions of the wall material, support conditions, window geometry, and other properties. With these real functions Eq. (B-5) can only be solved numerically as done by Wiehle and Bockholt.[1] However, for illustrative purposes and for drawing the form of similarity rules, we assume below: (1) the loading and deflection distributions are independent of window geometry and location, and (2) the resistance function $q(y) = ay$ where a is the ratio of ultimate resistance to the corresponding ultimate deflection. The initial conditions for Eq. (B-5) are that the wall is at rest $\dot{y} = 0$ and flat $y = 0$ at time $t = 0$. Defining the scaled parameters,

$$\delta^2 \equiv a\left(\frac{2V_c}{A\Delta}\right)^2 \frac{g}{\rho_w T_w}(P_{so} - P_o) \quad \text{and} \quad \Omega \equiv \left(\frac{2V_c}{A\Delta}\right)^2 \frac{g}{\rho_w T_w^2}(P_{so} - P_o)^2 \qquad \text{(B-6)}$$

and nondimensional deflection and time

$$\eta \equiv \frac{y}{T_w} \qquad \tau = \frac{t}{\frac{2V_c}{A\Delta}(P_{so} - P_o)^{1/2}}$$

the problem at hand reduces with Eq. (B-3), to

$$\left.\begin{aligned} \ddot{\eta} + \beta^2\eta &= \Omega(1-\tau)^2 \\ \eta(0) &= 0 \quad \dot{\eta}(0) = 0 \end{aligned}\right\} \tag{B-7}$$

The solution involves a quadratic function of time upon which a harmonic oscillator is imposed.

$$\frac{\beta^2\eta}{\Omega} = \frac{(\beta^4+4)^{1/2}}{\beta^2}\ \text{Cos}\ (\beta\tau + C_2) + (1-\tau)^2 - \frac{2}{\beta^2} \tag{B-8}$$

where the frequency constant $C_2 = \text{ArcCos}\left[\pm 2/(\beta^4+4)^{1/2}\right]$.

Differentiating Eq. (B-8) and eliminating τ, the magnitudes of deflection, velocity, and acceleration may be obtained. At collapse, set the criterion $\eta = 1$ to obtain time of collapse and velocity at collapse as functions of Ω and β.

Thresnoid conditions (*) of collapse are given by collapse with zero velocity so that $\Omega^* = \Omega^*(R)$ and $\tau^* = \tau^*(R)$. Noting from Eq. (B-6) that $\beta^2/\Omega^{\frac{1}{2}} \propto V_c/A$ and $\Omega/\beta^2 \propto (P_{so} - P_o)$, Figure B-1 shows the collapse threshold conditions thus predicted. For overpressures exceeding the threshold overpressure, the time of collapse will be shorter than τ^* and velocity at collapse will be larger than zero.

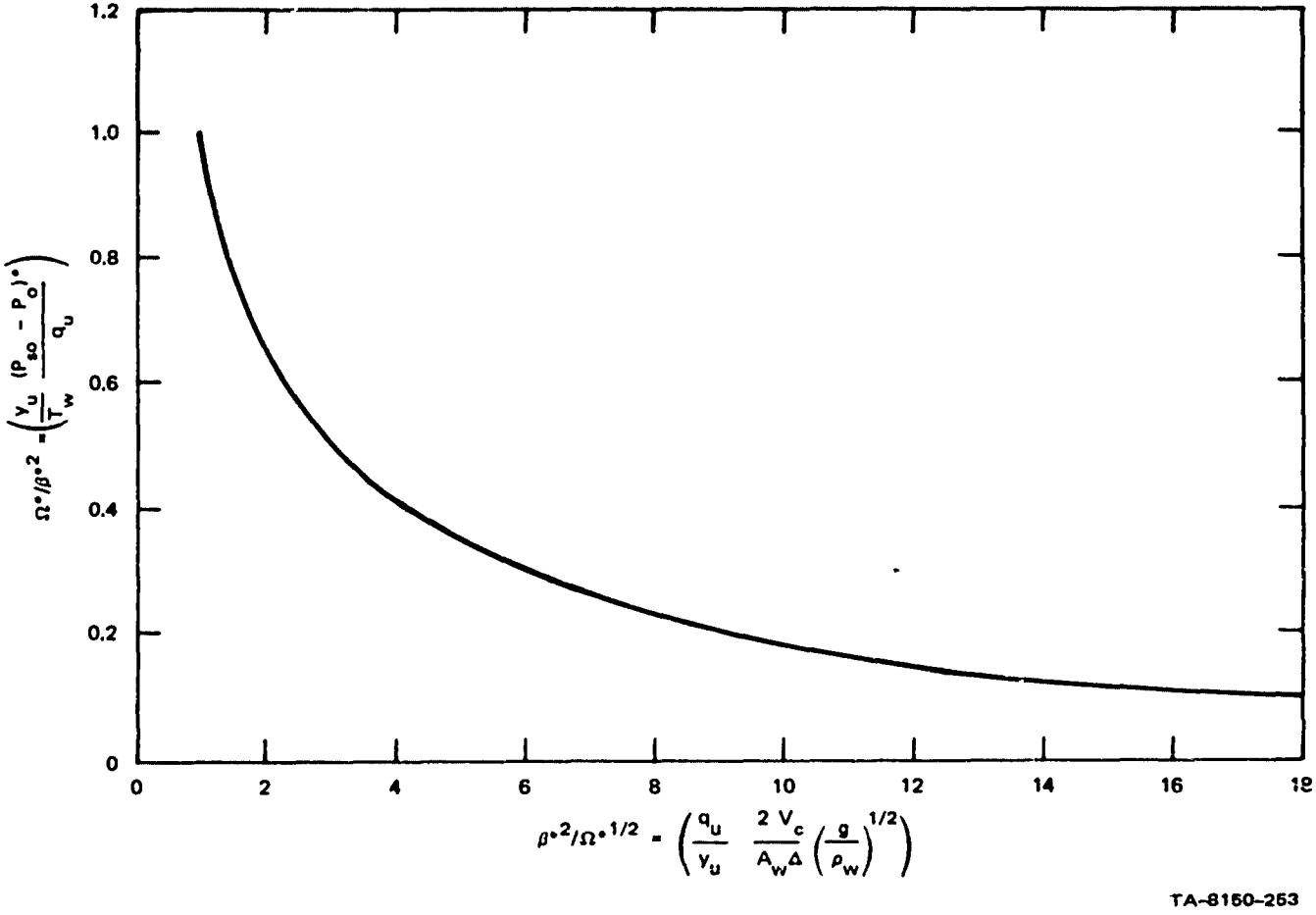

FIGURE B-1 COLLAPSE OVERPRESSURE AS A FUNCTION OF CHAMBER PROPERTIES

4. Concluding Comments

The analyses described here successfully delineate the variables of the problem to arrive at the following scale variables:

(1) Room-filling process

- Independent variables
  - Elapsed time after shock incidence

$$\tau \equiv t \Big/ \frac{2V_c}{A\ell} (P_{so} - P_o)^{1/2}$$

  - Positive-phase duration

$$\tau_+ \equiv t_+ \Big/ \frac{2V_c}{A\ell} (P_{so} - P_o)^{1/2}$$

- Dependent variables
  - Pressure

$$\pi \equiv (P_e - P_c) \Big/ (P_{so} - P_o)$$

  - Filling time

$$\tau_f \equiv t_f \Big/ \frac{2V_c}{A\ell} (P_{so} - P_o)^{1/2}$$

(2) Flow in the room

- Independent variables
  - Distance

$$\xi \equiv \frac{64C'}{3} \frac{x}{w}$$

  - Radius

$$\Psi \equiv 2r/w$$

- Time

$$\tau \equiv t \Big/ \frac{2V_c}{A\ell} (P_{so} - P_o)^{1/2}$$

- Dependent variables
  - Velocity

$$U \equiv u \Big/ C_d \left[\frac{2g}{\rho} \frac{\gamma}{\gamma-1} (P_{so} - P_o) \right]^{1/2}$$

  - Entrainment

$$V \equiv v \Big/ C_d \left[\frac{2g}{\rho} \frac{\gamma}{\gamma-1} (P_{so} - P_o) \right]^{1/2}$$

  - Potential core length

$$\xi_c \equiv \frac{64C'}{3} \frac{x_c}{w}$$

  - Potential core width

$$\psi_c \equiv 2r_c / w$$

  - Jet diameter

$$\psi_{max} \equiv 2\delta / w \quad .$$

(3) Collapse dynamics

- Independent variables
  - Time

$$\tau \equiv t \Big/ \frac{2V_c}{A\ell} (P_{so} - P_o)^{1/2}$$

- Resistance-inertia ratio

$$\beta^2 \equiv a\left(\frac{2V_c}{A\Delta}\right)^2 \frac{g}{\rho_w T_w}\,(P_{so} - P_o)$$

- Total load, inertia ratio

$$\Omega \equiv \left(\frac{2V_c}{A\Delta}\right)^2 \frac{g}{\rho_w T_w^2}\,(P_{so} - P_o)^2 \quad .$$

- Dependent variables

  - Deflection

$$\eta \equiv \frac{y}{T_w}$$

  - Velocity

$$\dot{\eta} \equiv \frac{dy}{dt} \cdot \frac{2V_c}{A\Delta}\,(P_{so} - P_o)^{1/2} \cdot \frac{1}{T_w}$$

  - Acceleration

$$\ddot{\eta} \equiv \frac{d^2y}{dt^2}\left(\frac{2V_c}{A\Delta}\right)^2 (P_{so} - P_o) \cdot \frac{1}{T_w}$$

  - Collapse threshold values of

$$\Omega^*,\ \beta^{*2},\ \tau^*,\ \ddot{\eta}^*$$

  - Collapse τ, $\dot{\eta}$ and $\ddot{\eta}$.

REFERENCES

1. C. K. Wiehle and J. L. Bockholt, "Description of Analytical Procedures for the Evaluation of Existing Structures," Technical Report for DCPA, Stanford Research Institute, Menlo Park, California (June 1972).

2. J. F. Melichar, "The Propagation of Blast Waves into Chambers," BRL-MR 1920, Ballistic Research Laboratories, Aberdeen Proving Ground, Maryland (March 1968).

3. A. H. Shapiro, The Dynamics and Thermodynamics of Compressible Fluid Flow (The Ronald Press Company, New York, New York, 1953).

4. A. R. Kriebel, "Airblast in Tunnels and Chambers," URS 7050-2, Final Report for DCPA, URS Research Corporation, Burlingame, California (February 1972).

5. H. Schlicting, Boundary-Layer Theory (McGraw-Hill, New York, New York, 1968).

Appendix C

MODIFICATION OF THE LONGINOW DEBRIS MODEL AND ITS USE IN EVALUATING PARAMETRIC SENSITIVITY

By

Steve J. Wiersma

Appendix C

MODIFICATION OF THE LONGINOW DEBRIS MODEL AND ITS USE IN EVALUATING PARAMETRIC SENSITIVITY

The Longinow debris model* was modified for use in predicting the trajectories and final location of objects of specified physical characteristics and initial conditions that were hit by a blast wave. The ultimate objective for our use of the debris model was to locate the debris in the hypothetical target area for a specified attack situation that was developed in Appendix A.

The computer program calculates the trajectories of the fragments of a wall section after it is collapsed by a blast wave. The wall section may be the exterior wall of one room of a high-rise building (see Figure C-1). Assumptions made in the model are the following:

(1) The wall section is hit by the free-field airblast that is traveling perpendicularly to the wall.

(2) At a specified incipient collapse pressure at which the midpoint of the wall has been displaced by an amount equal to the thickness of the wall, the wall breaks into four fragments (whose geometric dimensions are shown in Figure C-1) and these fragments retain their shape until they hit the ground.

(3) The wall is homogeneous.

(4) The wall fragments are acted on only by gravity and the surrounding air after the wall collapse until they hit the ground and do not interact with other fragments or with noncollapsed portions of structures.

(5) The wall fragments have initial velocities which depend on the ratio of the peak overpressure of the blast to the collapse overpressure of the wall.

(6) The wall fragments are rotated by the action of the blast wave and thus start in a position to experience lift and also have initial angular momentum.

*A. Longinow, G. Ojdrovich, L. Bertram, and C. Wiedermann, "People Survivability in a Direct Effects Environment and Related Topics," OCPA Work Unit 1614D, Final Report, IIT Research Institute, Chicago, Illinois (May 1973).

The trajectories of wall fragments for six cases were computed from the time of wall collapse until the fragments hit the ground. A summary of the dynamic properties of the top fragment (the shaded fragment in Figure C-1) for each of the six cases is given in Table C-1, Numbers 1 through 6. The trajectory of the center of mass of the fragment for each case is shown in Figures C-2 and C-3. End views of the fragment to show the rotation of the fragment are plotted for three of the cases in Figure C-2. End views are not shown for the cases plotted in Figures C-3 because the vertical and horizontal scales are different; however, the angle of rotation at the time the fragment reaches the ground can be found in Table C-1.

In all six cases analyzed, the wall section is 15.75 by 8.83 feet and has its bottom edge located 33 feet above the ground, corresponding to a typical fourth-floor room. (The trajectories for fragments of walls on lower floors can be found from the plots by shifting the vertical axis.) Two different wall compositions were analyzed: a 4-inch-thick wall with a mass of 1.51 slugs per square foot of wall area and a 6-inch-thick wall with a mass of 0.272 slugs per square foot of wall area. The heavier wall composition corresponds to a brick wall and the lighter composition corresponds to a plaster board, wood-siding wall with 2- by 4-inch studs. The incipient collapse overpressure is 1.5 psi in all cases. Each wall composition is evaluated for peak overpressures of 2, 5, and 10 psi from the blast wave of a 5-MT weapon.

The trajectory of the fragment for all six cases is also calculated without considering rotation of the fragment* so that the sensitivity of the trajectory to rotation of the fragment can be determined. A summary of these calculations is given in Table C-1, Numbers 1a to 6a. In these calculations the horizontal and vertical accelerations of the fragment are respectively:

*When the fragment is not rotated, there are no lift forces on the fragment.

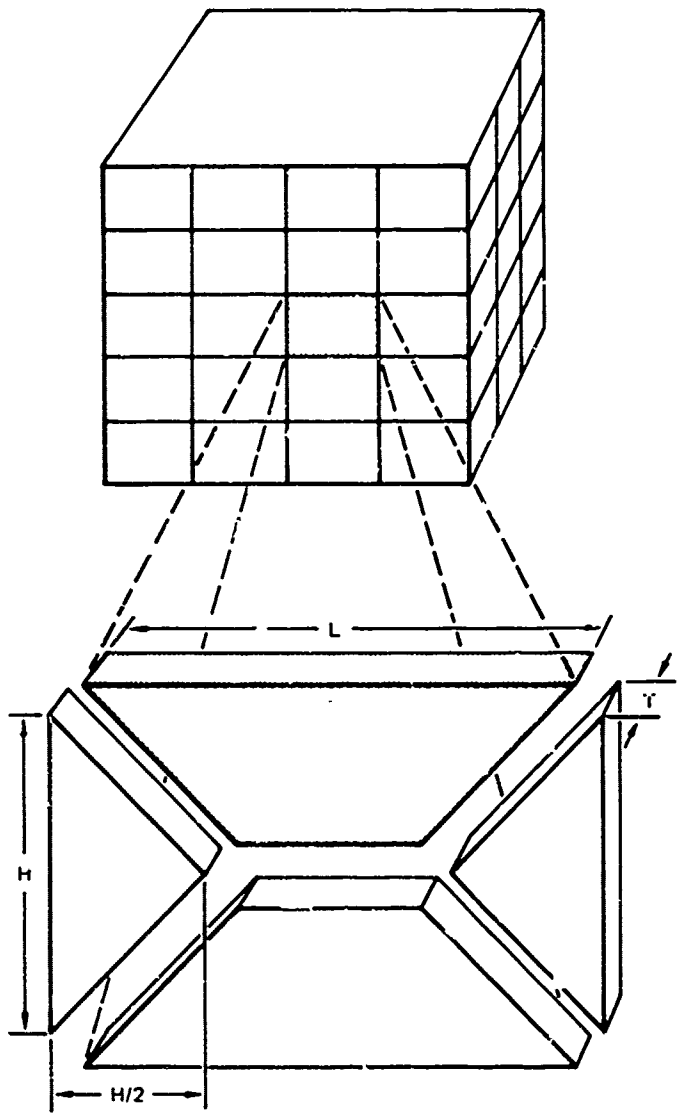

FIGURE C-1 HYPOTHESIZED WALL SECTION COLLAPSE PATTERN

Table C-1

SUMMARY OF THE DYNAMIC PROPERTIES OF THE TOP FRAGMENT OF A WALL SECTION COLLAPSED BY A BLAST WAVE

No.	T (in.)	M/A (slugs ft^{-2})	ΔP (psi)	P_c (psi)	Z (ft)	t (sec)	Y (ft)	V_z ($ft\ sec^{-1}$)	V_y ($ft\ sec^{-1}$)	θ (deg)
1	4	1.51	2	1.5	39.9	1.55	10.8	46.6	11.6	13
2	4	1.51	5	1.5	39.9	1.74	59.6	44.6	50.4	31
3	4	1.51	10	1.5	39.9	2.16	242	44.2	144.0	29
4	6	0.272	2	1.5	39.9	1.67	46.0	45.9	44.0	17
5	6	0.272	5	1.5	39.9	2.21	221	46.0	124.5	36
6	6	0.272	10	1.5	39.9	--	--	--	--	--
1a	4	1.51	2	--	39.9	1.52	9.5	49.1	8.7	0
2a	4	1.51	5	--	39.9	1.52	50.6	49.1	48.0	0
3a	4	1.51	10	--	39.9	1.52	163.6	49.1	162.5	0
4a	6	0.272	2	--	39.9	1.52	53.2	49.1	48.6	0
5a	6	0.272	5	--	39.9	1.52	282	49.1	268	0
6a	6	0.272	10	--	39.9	1.52	913	49.1	906	0

T - wall thickness

M/A - mass of fragment divided by fragment area

ΔP - peak overpressure of blast

P_c - collapse overpressure of wall

Z - height of center of mass of fragment at moment of collapse

t - time after collapse for fragment to hit ground

Y - horizontal distance traveled by fragment before it hits ground

V_z - downward velocity of fragment when it hits ground

V_y - horizontal velocity of fragment when it hits ground

θ - angle through which fragment has rotated before it hits ground.

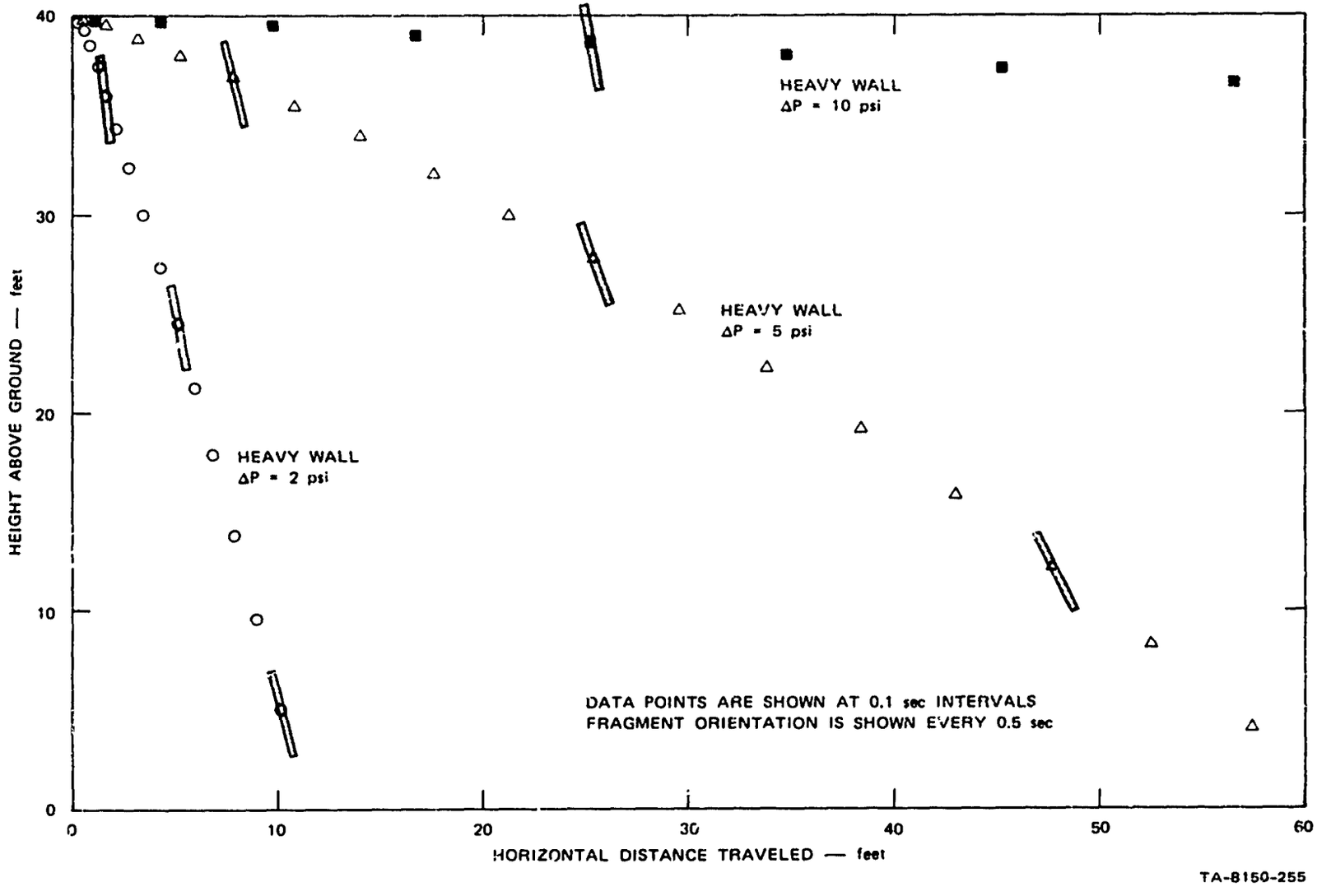

FIGURE C-2 TRAJECTORIES OF THE TOP FRAGMENT OF A HEAVY WALL WHICH IS COLLAPSED BY A BLAST WAVE

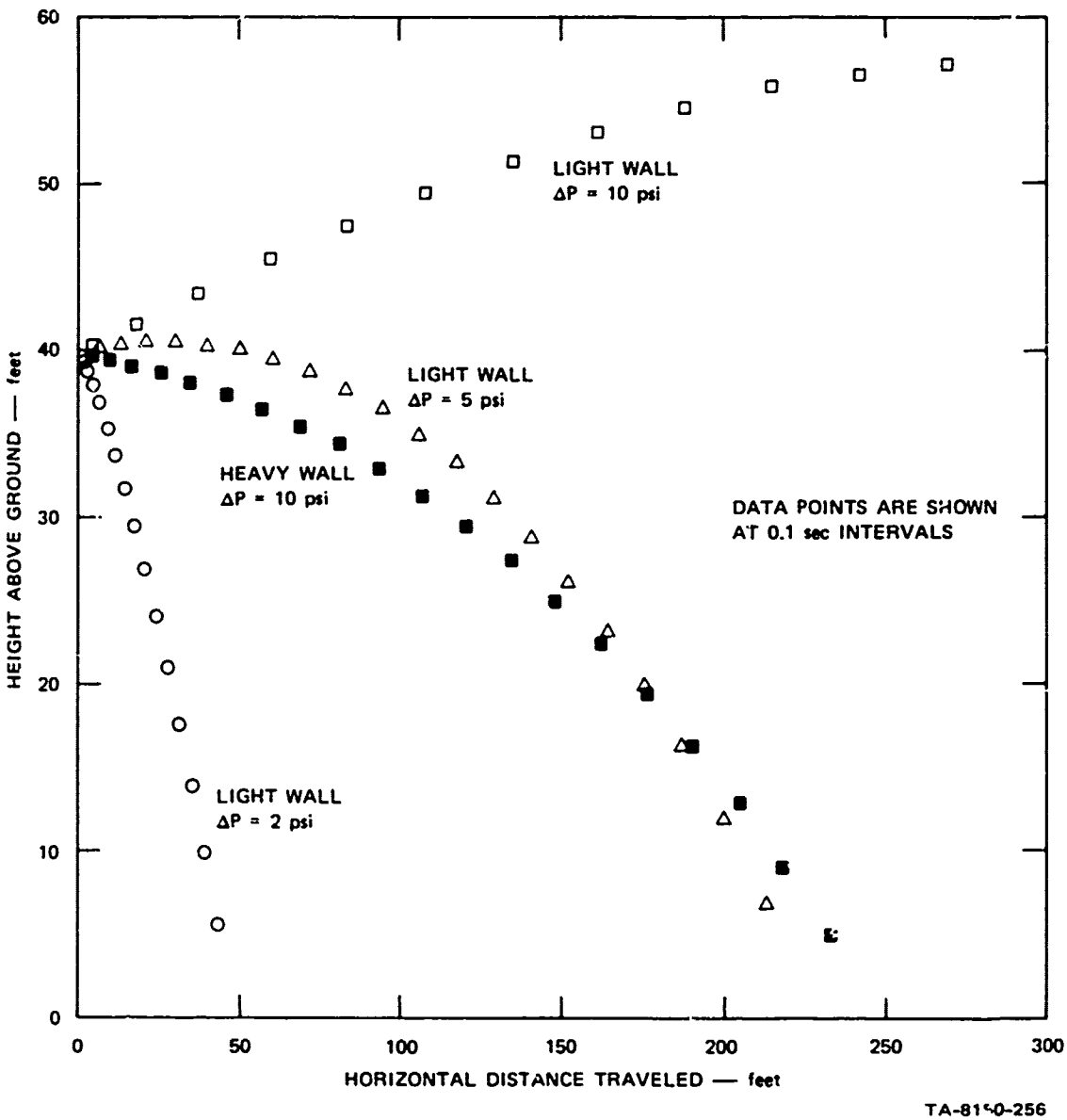

FIGURE C-3 TRAJECTORIES OF THE TOP FRAGMENT OF A WALL WHICH IS COLLAPSED BY A BLAST WAVE

$$A_y = \frac{A\,q(t)}{M} \quad ; \quad A_z = -g$$

where A is the area of the wall; M is the mass of the wall; q(t) is the dynamic pressure of the blast wave, which is a function of time; and g is the gravitational acceleration.

As can be seen in a comparison of Cases 1a through 6a and Cases 1 through 6 in Table C-1, the horizontal distance traveled before the fragment hits the ground and the horizontal velocity of the fragment at the time it hits the ground become very dependent on the rotation of the fragment as the peak overpressure is increased or as the mass per wall area is decreased. And in all of our cases the rate of rotation of the fragment is small; for higher rates of rotation the effect of rotation on the position and velocity of the debris when it hits the ground would be greater.

Our computations stopped when the fragment hit the ground. Of course, the fragments will continue to bounce and tumble and will probably break up into many smaller pieces after they hit the ground. Longinow estimated the soil-spring coefficients and the breakup pattern of the fragments when they hit the ground in his debris model and continued to compute fragment trajectories after contact with the ground*; however, he did not explore the sensitivity of the results to these input variables.

Applying the debris model to a specific attack situation in a hypothetical target area is an overwhelming task because of the deterministic nature of the model. Each particle's motion must be calculated as the model avoids any treatment of randomizing processes. The input statistics needed are overwhelming, and their values are currently subject to large

---

*Longinow et al.

errors. For example, it was just shown that the amount of rotation of a wall fragment critically influences where its debris will land. The mechanics of wall collapse are not easily determined; therefore the estimate of the rotation of wall fragment used in the debris model is subject to large errors. Interaction of fragments probably also critically influences the deposit of debris, but treating interaction of fragments is not now within the state of the art of the debris model. Two other shortcomings of the debris model are that the objects are loaded by the free-field blast wave and that only a blast wave traveling perpendicularly to the face of an object can be treated. Only under very specialized cases would the free-field blast wave act on a wall, for example, as room filling processes would greatly alter the blast wave loading.

The state of the art allows us only to explore the sensitivity of the results to the various input variables in the hope of obtaining a better understanding of how the initial state of debris depends on the blast wave that generates it. It is not possible to use the debris model at present to locate with any confidence the debris in a target area in an attack situation.

Appendix D

A SIMPLE COMPUTER PROGRAM FOR ESTIMATING URBAN FIRE STARTS FOLLOWING A NUCLEAR EXPLOSION

By

Stanley B. Martin

Appendix D

A SIMPLE COMPUTER PROGRAM FOR ESTIMATING URBAN FIRE STARTS FOLLOWING A NUCLEAR EXPLOSION

This program makes use of an equation originally proposed by John and Passel[1] and subsequently developed into an analytical procedure at URS[2] to estimate the frequency-spatial distribution of initial structural fires in a given urban use (or occupancy) class. In its simplest form, the equation predicts the probability that a room (on a given floor in a building of given occupancy) whose windows are exposed to the thermal radiation from the fireball will suffer a fire that, if left unattended, will cause the room to become fully engulfed in fire. This equation,

$$P_r = 1 - \exp\left[-\sum_i \mu_i \rho_{e,i} \rho_{f,i}\right] \quad ,$$

in which i represents the classes of fuels making up the contents of the room, may be usefully approximated by:

$$P_r \simeq 1 - \exp\left[-\rho_{e,\pm 1}\left(\mu_{+1} + \mu_{-1}\rho_{f,-1}\right) - \mu_o \rho_{f,o}\right]$$

where

$\rho_{e,i}$ = the probability of exposure of the room contents, excluding the window coverings (assumed to be a constant much smaller than unity)

$\rho_{f,i}$ = the probability that a fuel in the ith class, once ignited, will support a fire that will lead to total room involvement

μ_i = the mean number of fuels in the ith class that will be ignited if exposed .

The subscripts i = +1, i = -1, and i = 0 refer to the classes of fuels that, respectively:

(1) (i = +1) represents contents, excluding window coverings, for which $\rho_{f,i}$ is near unity.

(2) (i = -1) represents room contents (not window coverings), for which $\rho_{f,i}$ is much less than unity.

(3) (i = 0) represents window coverings (for which $\rho_{e,i}$ is assumed to be unity).

The rationale underlying this approximation and the choice of values for the component probabilities are described in Ref. 3.

The mean number of ignitable fuels in each class is a sequenoidal, monotonically increasing function of the radiant energy, Q, to which they are exposed. The mean-number function, $\mu_i(Q)$, may be expressed nondimensionally as:

$$\frac{\mu_i(Q)}{M_i} = \left[1 + \frac{(B_i + 1)}{(B_i - 1)} \left(\frac{Q}{Q_{infl}}\right)^{-B_i}\right]^{-1} ,$$

where M_i, representing the total count of fuels in the ith class, like the empirical constant B_i, depends only on the fuel class and occupancy, and Q_{infl}, the value of radiant exposure at the inflection point in the mean-number function, is also a function of the conditions of burst and may be used to extrapolate from one situation to another. The mean-number coefficients, M_i, B_i, and Q_{infl}, for the three fuel classes and occupancies treated in the program are based on survey data (for a summary, see Ref. 4)

and represent ignition thresholds for a 5-MT airburst at 2.74 miles height of burst (HOB), (referred to in the program as the reference yield and HOB).

The program makes use of the empirical relationship (from Ref. 2),

$$Q_{infl}\,(W,HOB) = Q_{infl}\,(5,2.74)\left(\frac{W}{5}\right)^{0.143} \times \left(\frac{HOB}{2.74}\right)^{-0.021} \exp\,[0.297(2.74 - HOB)] \quad ,$$

to extrapolate the mean-number distribution from the reference conditions to the desired burst conditions.

Horizontal distances (in miles) from ground zero, D(k), corresponding to the chosen peak overpressures, P(k) (in psi), for which analytical results are to be given are estimated from:[5]

$$D(k) = 6(1 \pm \alpha)\,(W)^{1/3} / \{\sqrt{P(k)} - 0.02\,[\sqrt{P(k)} - 4]^2\} \quad .$$

For surface bursts the factor α equals zero. For low airbursts (below the "knee" of the overpressure-HOB curves), α is adequately approximated by:

$$\alpha = \frac{0.18\,H^*}{1 + \log_{10} P(k)}$$

where H^* is the burst height expressed in fireball radii. This expression is simply a straightline approximation of the lower portion of the HOB curves.

Radiant exposures are computed from slant distances rather than from horizontal distances. The slant distance (in miles) is simply:

$$S(k) = \sqrt{D(k)^2 + H^2} \quad ,$$

where H represents the effective radiating height of the fireball (in miles), which is assumed to be equivalent to the burst height for airbursts and one-third of the fireball radius for surface bursts. The free-field radiant exposure (in cal cm^{-2}) for a visibility V (in miles) is estimated from:

$$Q(k) = 1040W \left[1 + 1.4S(k) / V\right] \exp\left[-2S(k)/V\right] / S(k)^2 \quad .$$

The attenuating effect of the artificial horizon is approximated by simple geometric considerations if any portion of the fireball is obscured.

A listing of the program (written in Super Basic) is reproduced on the following pages.

BLASTFIRE PROGRAM LISTING

```
1 !BLASTFIRE
2 ! THIS PROGRAM ESTIMATES PROBABILITIES OF SIGNIFICANT ROOM FIRES
3 ! FOR 3 DIFFERENT OCCUPANCIES AND VARYING DISTANCES FROM GZ,
4 ! REPRESENTING VARYING BLAST OVERPRESSURES.
5 ! REQUIRED DATA ARE COEFFICIENTS OF MEAN-NUMBER FUEL DISTRIBUTIONS
6 ! FOR MAJOR (DENOTED I=+1) AND MINOR (DENOTED II=-1) ROOM CONTENTS
7 ! AND FOR WINDOW COVERINGS (DENOTED I=0) ALONG WITH THE INFLECTION-
8 ! POINT RADIANT EXPOSURES FOR A SPECIFIED YIELD AND BURST HEIGHT.
9 ! THESE DATA ARE ENTERED INTO STATEMENTS 900-909 AS FOLLOWS:
10! REFERENCE YIELD (IN MT) FIRST, REFERENCE HOB (IN MILES) SECOND,
11! THEN BY THE M,B,&Q-INFLECTION VALUES FOR RESIDENCES (ORDERED
12! -1,0,+1), FOLLOWED BY THOSE FOR COMMERCIAL OCCUPANCIES, AND LAST
13! BY THOSE FOR INDUSTRIAL OCCUPANCIES. DATA STATEMENT 910 CONTAINS
14! THE NUMBER OF BLAST OVERPRESSURES FOR WHICH THE PROBABILITIES ARE
15! CALCULATED FOLLOWED BY THE OVERPRESSURE VALUES.
30 DIM A(-1:1),P(20),F(-1:1,20),F$(-1:1,20),S(20)
   DIM P$(20),D(20),Q(20),E$(-1:1,3),M(-1:1,3),B(-1:1,3),Q$(-1:1,3)
32 DIM C(-1:1,3),M$(-1:1,3,20),U(3,20),U$(3,20),V(3,20),V$(3,20)
33 DIM W(3,20),W$(3,20),Y$(3,20),Z$(3,20),E(-1:1,3,20),X(20),Y(20)
34 DIM A$(20),C$(20)
40 A(-1)=.5,A(0)=.8,A(1)=.5
45 READ WO,HO ! REFERENCE VALUES
50 FOR J=1TO3 ! REFERS TO OCCUPANCY
55 FOR I=-1,0,1 ! REFERS TO FUEL CLASS
60 READM(I,J),B(I,J),Q$(I,J) ! COEFFICIENTS OF DISTRIBUTION
65 NEXTI
70 NEXTJ
75 PRINT"WHAT YIELD (IN MT)";
80 INPUT W1
85 W3=W1↑(1/3)
90 PRINT"IF SURFACE BURST, TYPE 0; IF AIRBURST, 1";
95 INPUT H
100 PRINT"WHAT IS VISIBILITY (IN MILES)";
105 INPUT V1
110 READ N
115 FOR K=1TON
120 READ P(K)
125 F(1,K)=1,F(-1,K)=0.01,F(0,K)=0.01
130 F$(1,K)=1,F$(-1,K)=0,F$(0,K)=0
135 IFP(K)<2THENF$(-1,K)=.01,F$(0,K)=.01ELSE IFP(K)>5THENF$(1,K)=.5
   ELSE F$(1,K)=(8-P(K))/6
140 P$(K)=SQRT(P(K))
```

```
145 D(K)=6*W3/(P$(K)-.02*(P$(K)-4)↑2)
155 NEXTK
160 IF H=0 THEN GOSUB1000 ELSE GOSUB2000
165 G="%%%.%% %%%.%%  %%%%.%  %.%%%%%  %.%%%%%  %.%%%%%    %.%%%%%"
166 L="       %%%.%%  %%%.%%  %.%%%%%  %.%%%%%  %.%%%%%    %.%%%%%"
170 FORJ=1TO3
171 IF J=1 THEN175
172 IF J=2 THEN177
173 PRINT"      INDUSTRIAL OCCUPANCY"
174 GOTO180
175 PRINT"      RESIDENTIAL OCCUPANCY"
176 GOTO180
177 PRINT"       COMMERCIAL OCCUPANCY"
180 E$(I,J)=.2 FOR I=1,-1
185 E$(I,J)=.1 FOR I=0
190 FOR I=-1,0,1
195 C(I,J)=(B(I,J)+1)/(B(I,J)-1)
200 FORK=1TON
205 IF Q(K)>0 THEN M$(I,J,K)=M(I,J)/(1+C(I,J)*(A(I)*Q(K)/Q$(I,J))↑
    -B(I,J)) ELSE M$(I,J,K)=0
210 NEXTK,I
215 FORK=1TON
220 U(J,K) =M$(I,J,K)*E$(I,J)*F$(I,J) FOR I=1
222 U$(J,K)=M$(I,J,K)*E$(I,J)*F (I,K) FORI= 1
224 V(J,K)=M$(I,J,K)*E$(I,J)*F$(I,K) FOR I=-1
226 V$(J,K)=M$(I,J,K)*E$(I,J)*F(I,K) FORI=-1
228 W(J,K)=M$(I,J,K)*E$(I,J)*F$(I,K) FORI=0
230 W$(J,K)=M$(I,J,K)*E$(I,J)*F(I,K) FORI=0
240 Y$(J,K)=1-EXP( U(J,K)-V(J,K)-W(J,K))
250 Z$(J,K)=1-EXP(-U$(J K)-V$(J,K)-W$(J,K))
260 NEXTK
270 PRINT"              WINDOWS UNCOVERED"
280 PRINT"  POP   D/RAD AN  Q/EL AN  +        -       W   PROB(NBE/BE)"
290 FORK=1TON
300 PRINT IN IMAGE G:P(K),D(K),Q(K),U$(J,K),V$(J,K),W$(J,K),,Z$(J,K)
301 PRINT IN IMAGE L:A$(K),C$(K),U(J,K),V(J,K),W(J,K),Y$(J,K)
310 NEXTK
311 PRINT
312 PRINT
313 PRINT
320 FORK=1TON
330 FORI=-1,1
335 E(I,J,K)=.2*M$(O,J,K)/M(O,J)
336 IF QS(O,J)>A(I)*Q(K) THEN GO TO 342
```

```
340 M$(I,J,K)=M(I,J)/(1+C(I,J)*(A(I)*Q(K)/(Q$(I,J)+1E03/(A(I)*
    Q(K)-Q$(O,J))))↑-B(I,J))
341 GOTO345
342 M$(I,J,K)=0
345 NEXT I
350 E(I,J,K)=1.0 FOR I=0
360 U (J,K)=M$ (I,J,K)*E(I,J,K)*F$(I,K) FOR I=1
362 U$ (J,K)=M$ (I,J,K)*E(I,J,K)*F(I,K) FOR I=1
364 V (J,K)=M$ (I,J,K)*E (I,J,K)*F$(I,K)FOR I=-1
366 V$(J,K)=M$(I,J,K)*E (I,J,K)* F(I,K) FOR I=-1
368 W(J,K)=M$(I,J,K)*E(I,J,K)* F$(I,K)FOR I=0
370 W$(J,K)=M$(I,J,K)*E(I,J,K)*F(I,K) FOR I=0
380 Y$(J,K)=1-EXP(-U(J,K)-V(J,K)-W(J,K))
390 Z$(J,K)=1-EXP(-U$(J,K)-V$(J,K)-W$(J,K))
400 NEXTK
410 PRINT "WINDOWS COVERED"
420 PRINT"  POP   D/RAD AN  Q/EL AN  +       -    W     PROB(NBE/BE)"
430 FORK=1TON
440 PRINT IN IMAGE G:P(K),D(K),Q(K),U$(J,K),V$(J,K),W$(J,K),,Z$(J,K)
441 PRINT IN IMAGE L:A$(K),C$(K),U(J,K),V(J,K),W(J,K),Y$(J,K)
450 NEXT K,J
451 PRINT
452 PRINT
453 PRINT
454 RESTORE
455 GOTO45
900 DATA 5,2.74
901 DATA 5,6,13,1,5,12,1.6,5.1,23
902 DATA 12,5.9,12,3,5,12,3,4.5,21
903 DATA 8.2,7,13.6,2,5,12,2.6,4.1,23
910 DATA 11,1,1.5,2,3,4,5,6,8,10,15,20
1000 R=.5*W1↑.35
1001 H2=.3*R
1002 FOR K=1TON
1005 S(K)=SQRT(D(K)↑2+H2↑2)
1007 Q(K)=1040*W1*EXP(-2*S(K)/V1)*(1+1.4*S(K)/V1)/S(K)↑2
1009 NEXTK
1010 PRINT" FIREBALL RADIUS= ";R;"MILES"
1020 PRINT" WHAT BURST HEIGHT (IN FIREBALL RADII)";
1021 PRINT
1022 PRINT
1030 INPUT H1
1031 PRINT
1032 PRINT
1033 PRINT
```

```
1040 H1=R*H1+H2
1050 F RJ= 1TO3
1055 FORI=-1,0,1
1060 Q$(I,J)=Q$(I,J)*((2*W1/WO)↑.143)*((H1/HO)↑-.021) *
     EXP(.295*(HO-H1))
1070 NEXTI,J
1080 PRINT"  WHAT IS THE ANGLE OF THE ARTIFICIAL HORIZON (IN DEGREES)"
1090 INPUT B$
1091 PRINT
1092 PRINT
1093 PRINT
1100 B$=PI*B$/180
1110 T$=TAN(B$)/R
1120 B$=180*B$/PI
1130 FORK=1TON
1140 X(K)=D(K)*T$
1150 IF X(K)>1 THEN Y(K)=0 ELSE Y(K)=SQRT(1-X(K)↑2)
1160 Q(K)=.6*Q(K)*(1-2*(X(K)*Y(K)+ATAN(X(K),Y(K)))/PI)
1161 X=R/D(K)
1162 A$(K)=ATAN(X)*180/PI  !ANGLE SUBTENDED BY RADIUS OF FIREBALL
1163 C$(K)=0
1170 NEXTK
1180 PRINT"SURFACE BURST OF";W1,"MT YIELD (BETA=";B$,")"
1190 RETURN
2000 R=.4*W1↑.35
2010 PRINT" FIREBALL RADIUS=";R;" MILES"
2020 PRINT" WHAT HEIGHT OF BURST (IN FIREBALL RADII)",
2030 INPUT H1
2031 PRINT
2032 PRINT
2033 PRINT
2040 H1=R*H1
2050 FORJ=1TO3
2060 FORI=-1,0,1
2070 Q$(I,J)=Q$(I,J)*((  W1/WO)↑.143)*((H1/HO)↑-.021)*
     EXP(.295*(HO-H1))
2080 NEXTI,J
2090 FORK=1TON
2100 D(K)=D(K)*(1+(.18*H1/R/(1+LGT(P(K)))))
2101 S(K)=SQRT(D(K)↑2+H1↑2)
2104 Q(K)=1040*W1*EXP(-2*S(K)/V1)*(1+1.4*S(K)/V1)/S(K)↑2
2105 X=R/SQRT(D(K)*D(K)-R*R)
2106 A$(K)=ATAN(X)*180/PI   !ANGLE SUBTENDED BY RADIUS OF FIREBALL
2107 X=H1/SQRT(D(K)*D(K)-H1*H1)
2108 C$(K)=ATAN(X)*180/PI   !ANGLE TO MIDDLE OF FIREBALL
2110 NEXTK
2120 PRINT"AIRBURST OF";W1;" MT YIELD AND ";H1;" MILE HOB"
2130 RETURN
```

SAMPLE PROGRAM

Program input - After RUN is typed, the program will ask for the input data. Input data are underlined below.

```
 RUN
WHAT YIELD (IN MT)   ? 5
IF SURFACE BURST, TYPE 0; IF AIRBURST, 1    ? 1
WHAT IS VISIBILITY (IN MILES)    ? 10
 FIREBALL RADIUS=     .702586     MILES
 WHAT HEIGHT OF BURST (IN FIREBALL RADII)      ? 1
```

Program output - The following data are given in the output:

POP	Peak overpressure in psi
D	Distance in miles from observed peak overpressure to the center of the fireball
RAD AN	The angle in degrees from the center of the fireball to the edge of the fireball
Q	The peak radiant flux from the fireball in cal cm^{-2} sec^{-1}
EL AN	The angle in degrees from the ground to the center of the fireball
+	The probability of a primary fire start in an exposed room from major room contents
-	The probability of a primary fire start in an exposed room from minor room contents
W	The probability of a primary fire start in an exposed room from window hangings
PROB NBE	The probability of a primary fire start in an exposed room when blast effects are not considered
PROB BE	The probability of a primary fire start in an exposed room when blast effects are considered

AIRBURST OF 5 MT YIELD AND .702586 MILE HOB

RESIDENTIAL OCCUPANCY

WINDOWS UNCOVERED

POP	D/RAD AN	Q/EL AN	+	-	W	PROB(NBE/BE)
1.00	14.76	3.8	.00000	.00000	.00000	.00000
	2.73	2.73	.00000	.00000	.00000	.00000
1.50	11.05	11.8	.00001	.00000	.00001	.00002
	3.65	3.65	.00001	.00000	.00001	.00002
2.00	9.12	22.7	.00024	.00007	.00019	.00050
	4.42	4.42	.00024	.00000	.00000	.00024
3.00	7.06	49.7	.01239	.00444	.00092	.01760
	5.71	5.71	.01239	.00000	.00000	.01238
4.00	5.94	80.6	.10274	.00935	.00099	.10693
	6.79	6.79	.10274	.00000	.00000	.09764
5.00	5.22	113.6	.23404	.00991	.00100	.21726
	7.74	7.74	.23404	.00000	.00000	.20867
6.00	4.70	147.8	.29203	.00998	.00100	.26141
	8.59	8.59	.29203	.00000	.00000	.25326
8.00	4.01	218.3	.31585	.01000	.00100	.27881
	10.09	10.09	.31585	.00000	.00000	.27083
10.00	3.55	289.7	.31901	.01000	.00100	.28108
	11.41	11.41	.31901	.00000	.00000	.27313
15.00	2.87	466.8	.31991	.01000	.00100	.28173
	14.18	14.18	.31991	.00000	.00000	.27379
20.00	2.48	638.1	.31998	.01000	.00100	.28178
	16.48	16.48	.31998	.00000	.00000	.27384

WINDOWS COVERED

POP	D/RAD AN	Q/EL AN	+	-	W	PROB(NBE/BE)
1.00	14.76	3.8	.00000	.00000	.00000	.00000
	2.73	2.73	.00000	.00000	.00000	.00000
1.50	11.05	11.8	.00000	.00000	.00009	.00009
	3.65	3.65	.00000	.00000	.00009	.00009
2.00	9.12	22.7	.00000	.00000	.00187	.00186
	4.42	4.42	.00000	.00000	.00000	.00000
3.00	7.06	49.7	.00000	.00000	.00920	.00915
	5.71	5.71	.00000	.00000	.00000	.00000
4.00	5.94	80.6	.00212	.00011	.00092	.01207
	6.79	6.79	.00141	.00000	.00000	.00141
5.00	5.22	113.6	.05227	.00503	.00999	.06507
	7.74	7.74	.02614	.00000	.00000	.02580
6.00	4.70	147.8	.19522	.00942	.01000	.19316
	8.59	8.59	.09761	.00000	.00000	.09300
8.00	4.01	218.3	.30651	.00998	.01000	.27855
	10.09	10.09	.15325	.00000	.00000	.14209
10.00	3.55	289.7	.31761	.01000	.01000	.28653
	11.41	11.41	.15881	.00000	.00000	.14684
15.00	2.87	466.8	.31985	.01000	.01000	.28812
	14.18	14.18	.15993	.00000	.00000	.14779
20.00	2.48	638.1	.31997	.01000	.01000	.28821
	16.48	16.48	.15999	.00000	.00000	.14785

COMMERCIAL OCCUPANCY

WINDOWS UNCOVERED

POP	D/RAD AN	Q/EL AN	+	-	W	PROB(NBE/BE)
1.00	14.76	3.8	.00000	.00000	.00000	.00000
	2.73	2.73	.00000	.00000	.00000	.00000
1.50	11.05	11.8	.00007	.00001	.00003	.00011
	3.65	3.65	.00007	.00001	.00003	.00011
2.00	9.12	22.7	.00142	.00030	.00056	.00227
	4.42	4.42	.00142	.00000	.00000	.00142
3.00	7.06	49.7	.04444	.01344	.00276	.05883
	5.71	5.71	.04444	.00000	.00000	.04347
4.00	5.94	80.6	.24762	.02297	.00298	.23933
	6.79	6.79	.24762	.00000	.00000	.21934
5.00	5.22	113.6	.46024	.02386	.00300	.38
	7.74	7.74	.46024	.00000	.00000	.3688
6.00	4.70	147.8	.54907	.02397	.00300	.43788
	8.59	8.59	.54907	.00000	.00000	.42252
8.00	4.01	218.3	.59051	.02400	.00300	.46071
	10.09	10.09	.59051	.00000	.00000	.44596
10.00	3.55	289.7	.59731	.02400	.00300	.46437
	11.41	11.41	.59731	.00000	.00000	.44971
15.00	2.87	466.8	.59969	.02400	.00300	.46564
	14.18	14.18	.59969	.00000	.00000	.45102
20.00	2.48	638.1	.59992	.02400	.00300	.46577
	16.48	16.48	.59992	.00000	.00000	.45115

WINDOWS COVERED

POP	D/RAD AN	Q/EL AN	+	-	W	PROB(NBE/BE)
1.00	14.76	3.8	.00000	.00000	.00000	.00000
	2.73	2.73	.00000	.00000	.00000	.00000
1.50	11.05	11.8	.00000	.00000	.00026	.00026
	3.65	3.65	.00000	.00000	.00026	.00026
2.00	9.12	22.7	.00000	.00000	.00560	.00558
	4.42	4.42	.00000	.00000	.00000	.00000
3.00	7.06	49.7	.00000	.00000	.02759	.02721
	5.71	5.71	.00000	.00000	.00000	.00000
4.00	5.94	80.6	.00763	.00032	.02977	.03701
	6.79	6.79	.00509	.00000	.00000	.00507
5.00	5.22	113.6	.12817	.01325	.02996	.15749
	7.74	7.74	.06408	.00000	.00000	.06207
6.00	4.70	147.8	.38345	.02285	.02999	.35357
	8.59	8.59	.19173	.00000	.00000	.17447
8.00	4.01	218.3	.57083	.02396	.03000	.46463
	10.09	10.09	.28542	.00000	.00000	.24830
10.00	3.55	289.7	.59376	.02400	.03000	.47678
	11.41	11.41	.29688	.00000	.00000	.25687
15.00	2.87	466.8	.59947	.02400	.03000	.47976
	14.18	14.18	.29974	.00000	.00000	.25899
20.00	2.48	638.1	.59989	.02400	.03000	.47998
	16.48	16.48	.29994	.00000	.00000	.25914

INDUSTRIAL OCCUPANCY

WINDOWS UNCOVERED

POP	D/RAD AN	Q/EL AN	+	-	W	PROB(NBE/BE)
1.00	14.76	3.8	.00000	.00000	.00000	.00000
	2.73	2.73	.00000	.00000	.00000	.00000
1.50	11.05	11.8	.00009	.00000	.00002	.00011
	3.65	3.65	.00009	.00000	.00002	.00011
2.00	9.12	22.7	.00133	.00004	.00037	.00174
	4.42	4.42	.00133	.00000	.00000	.00133
3.00	7.06	49.7	.03094	.00630	.00184	.03833
	5.71	5.71	.03094	.00000	.00000	.03047
4.00	5.94	80.6	.16339	.01555	.00198	.16550
	6.79	6.79	.16339	.00000	.00000	.15074
5.00	5.22	113.6	.33892	.01632	.00200	.30039
	7.74	7.74	.33892	.00000	.00000	.28746
6.00	4.70	147.8	.44018	.01639	.00200	.36781
	8.59	8.59	.44018	.00000	.00000	.35608
8.00	4.01	218.3	.50159	.01640	.00200	.40547
	10.09	10.09	.50159	.00000	.00000	.39443
10.00	3.55	289.7	.51409	.01640	.00200	.41286
	11.41	11.41	.51409	.00000	.00000	.40195
15.00	2.87	466.8	.51916	.01640	.00200	.41583
	14.18	14.18	.51916	.00000	.00000	.40498
20.00	2.48	638.1	.51977	.01640	.00200	.41618
	16.48	16.48	.51977	.00000	.00000	.40534

WINDOWS COVERED

POP	D/RAD AN	Q/EL AN	+	-	W	PROB(NBE/BE)
1.00	14.76	3.8	.00000	.00000	.00000	.00000
	2.73	2.73	.00000	.00000	.00000	.00000
1.50	11.05	11.8	.00000	.00000	.00017	.00017
	3.65	3.65	.00000	.00000	.00017	.00017
2.00	9.12	22.7	.00000	.00000	.00373	.00372
	4.42	4.42	.00000	.00000	.00000	.00000
3.00	7.06	49.7	.00000	.00000	.01839	.01823
	5.71	5.71	.00000	.00000	.00000	.00000
4.00	5.94	80.6	.00761	.00009	.01985	.02716
	6.79	6.79	.00507	.00000	.00000	.00506
5.00	5.22	113.6	.09548	.00808	.01997	.11621
	7.74	7.74	.04774	.00000	.00000	.04662
6.00	4.70	147.8	.28350	.01575	.01999	.27330
	8.59	8.59	.14175	.00000	.00000	.13216
8.00	4.01	218.3	.47400	.01639	.02000	39974
	10.09	10.09	.23700	.00000	.00000	.21101
10.00	3.55	289.7	.50809	.01640	.02000	.41986
	11.41	11.41	.25405	.00000	.00000	.22434
15.00	2.87	466.8	.51871	.01640	.02000	.42599
	14.18	14.18	.25935	.00000	.00000	.22845
20.00	2.48	638.1	.51968	.01640	.02000	.42655
	16.48	16.48	.25984	.00000	.00000	.22883

REFERENCES

1. F. I. John and T. O. Passel, "Evaluation of Nuclear Weapon Thermal Threat," OCD Work Unit 4311C, Stanford Research Institute, Menlo Park, California (August 1966).

2. Stanley B. Martin, Robert Ramstad, and Clifford Colvin, "Development and Application of an Interim Fire-Behavior Model," OCD Work Unit 2538C, Final Report, URS Research Corporation, Burlingame, California, (April 1968).

3. T. Goodale, "Effects of Air Blast on Urban Fires," OCD Work Unit 2534I, Final Report, URS Research Corporation, Burlingame, California (December 1970).

4. S. B. Martin, "The Role of Fire in Nuclear Warfare: An Interpretive Review of the Current Technology for Evaluating the Incendiary Consequences of the Strategic and Tactical Uses of Nuclear Weapons," DASA Report 2692, URS Research Corporation, Burlingame, California, (February 1971).

5. C. M. Haaland, Survive, Vol. 2, No. 2, p. 16 (1969).

Appendix E

FIRE PORTRAITS OF CAMP PARKS EXPERIMENTS 13 THROUGH 15

By

Steve J. Wiersma

Appendix E

FIRE PORTRAITS OF CAMP PARKS EXPERIMENTS 13 THROUGH 15

Data from Camp Parks Experiment 13, March 17, 1973

Data from Camp Park Experiment 14, April 28, 1973

Data from Camp Parks Experiment 15, April 23, 1973

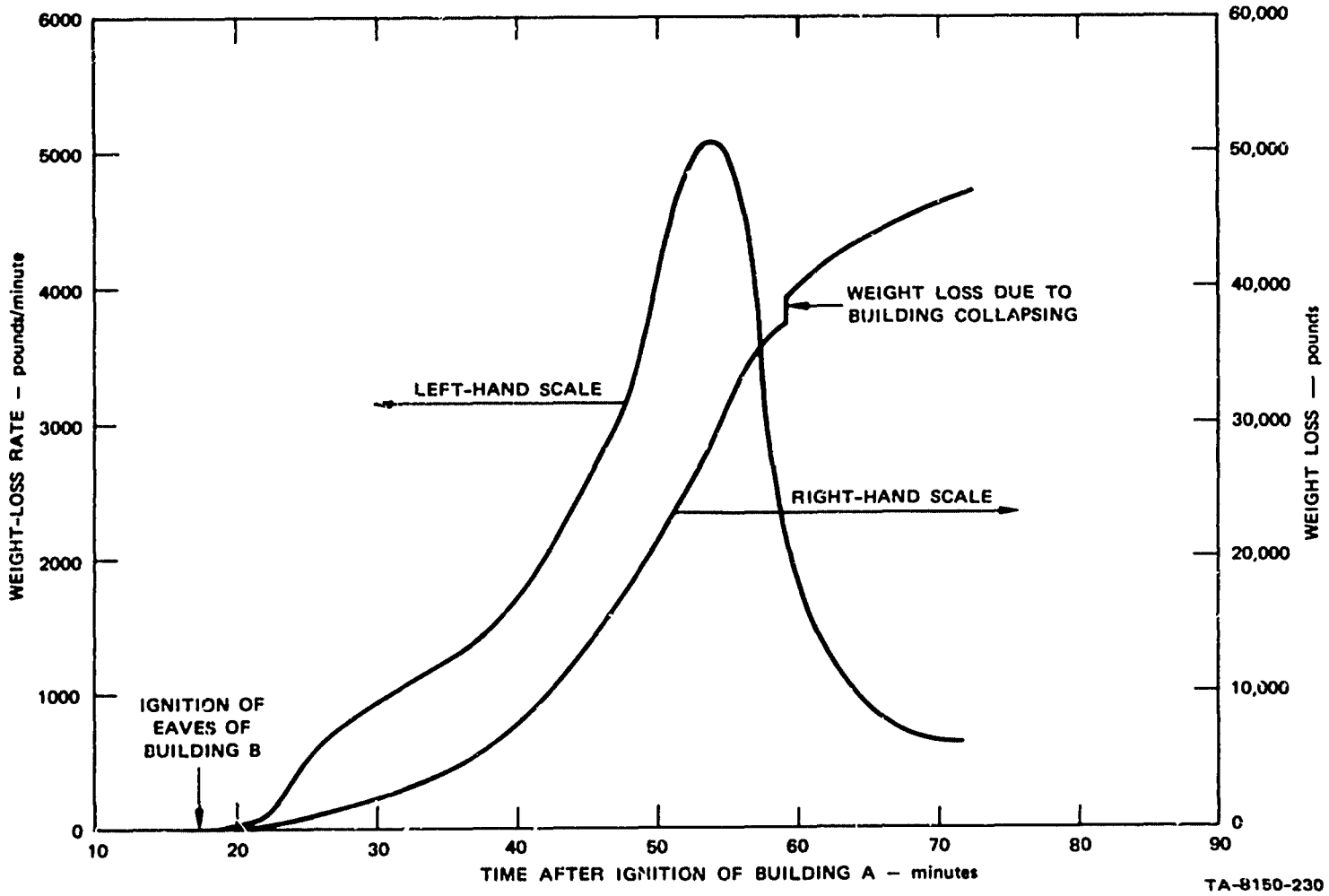

FIGURE E-1 WEIGHT LOSS AND WEIGHT-LOSS RATE FOR BUILDING B, CAMP PARKS EXPERIMENT 13

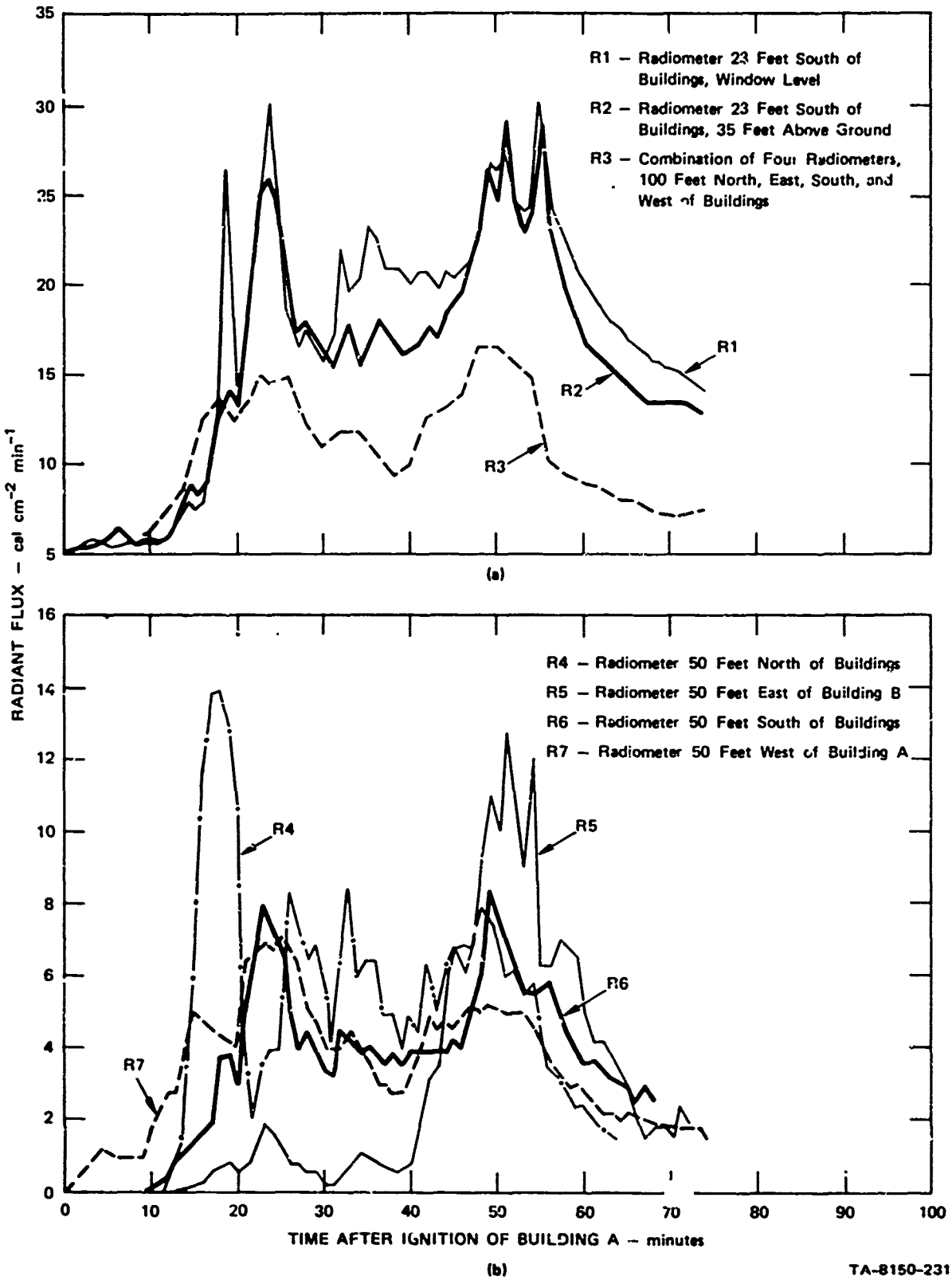

FIGURE E-2 RADIANT FLUX FIELD, CAMP PARKS EXPERIMENT 13

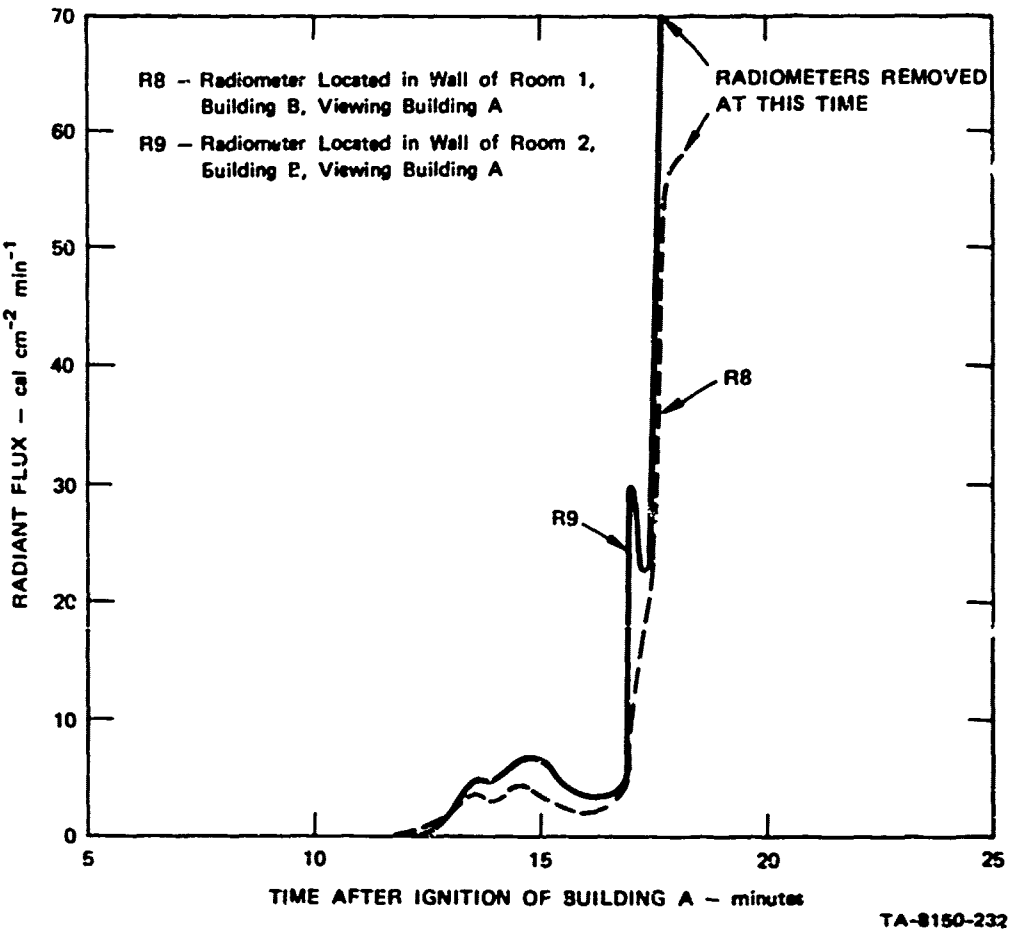

FIGURE E-3 RADIANT FLUX MEASUREMENTS, CAMP PARKS EXPERIMENT 13

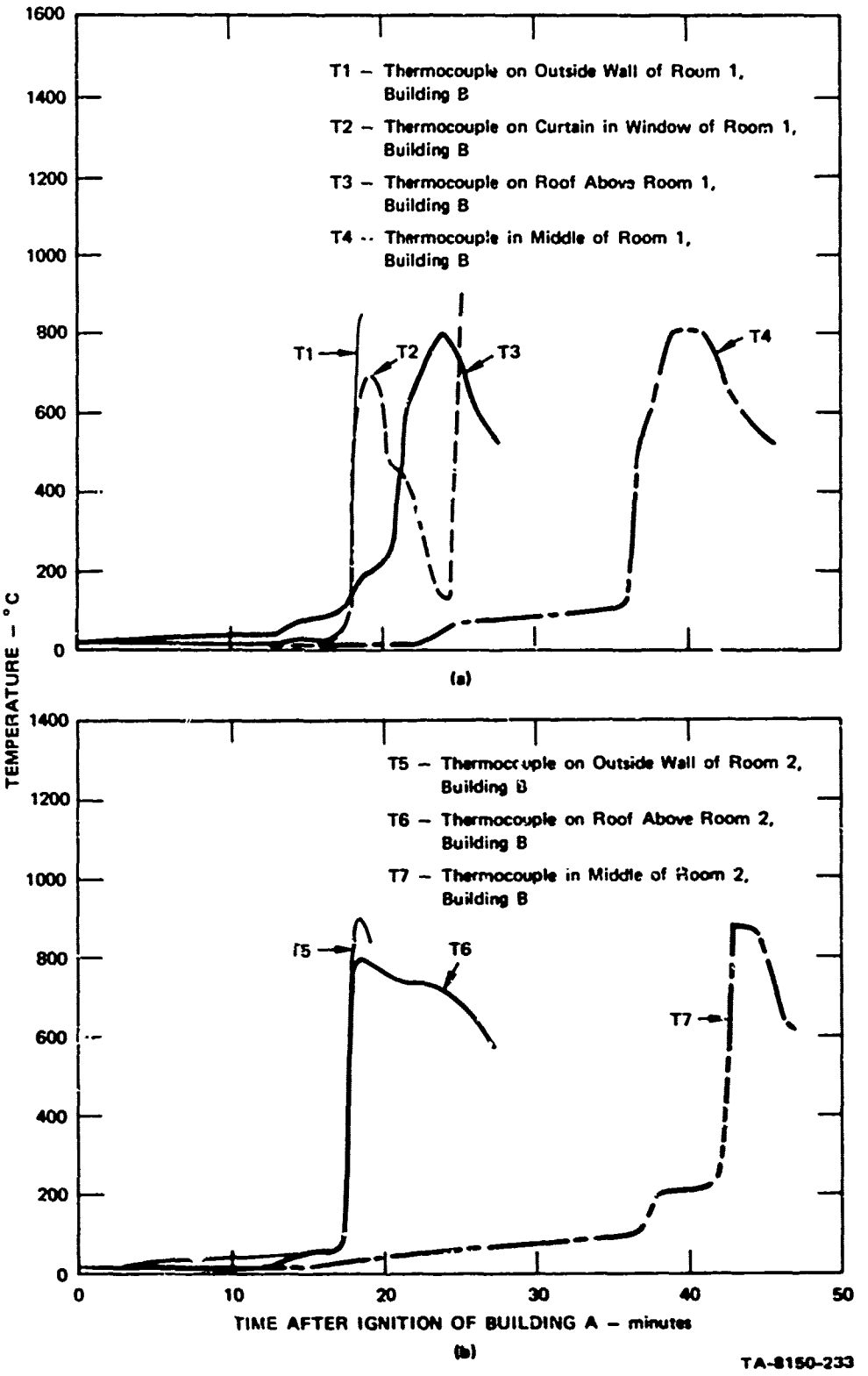

FIGURE E-4 TEMPERATURES, CAMP PARKS EXPERIMENT 13

Table E-1

FIRE SPREAD IN BUILDINGS A AND B, CAMP PARKS EXPERIMENT 13

Room Number	Time of String Break After Ignition of Building A (minutes)			
	Building A		Building B	
	Room	Attic Above Room	Room	Attic Above Room
1	1	7	38	31
2	7	11	40	35
3	12	21	34	32
4	19	13.5	40	22
5	15	10	44	42
6	11	12	40	28
7	20	12	40	27
8	19	13	39	28

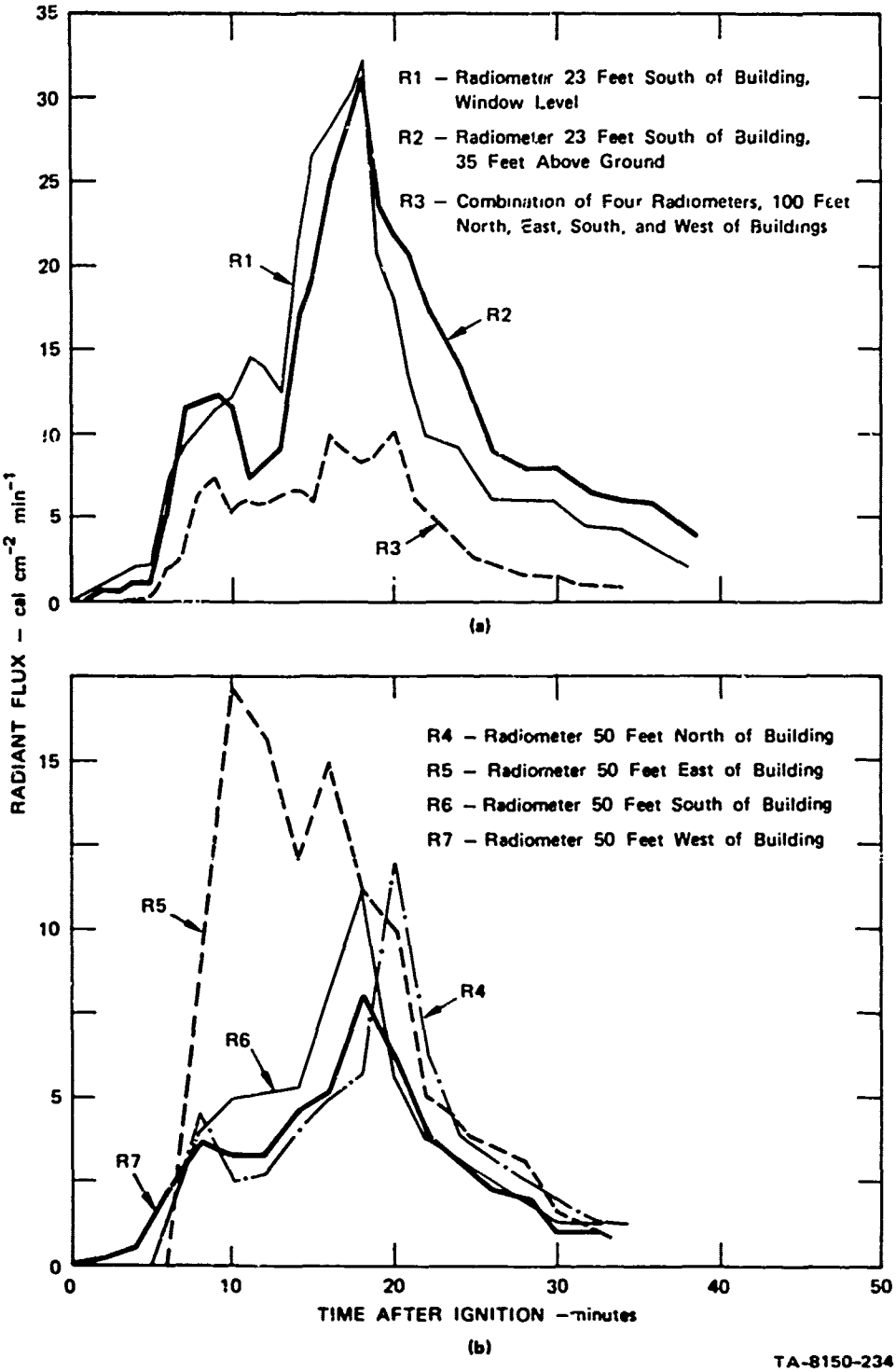

FIGURE E-5 RADIANT FLUX FIELD, CAMP PARKS EXPERIMENT 14

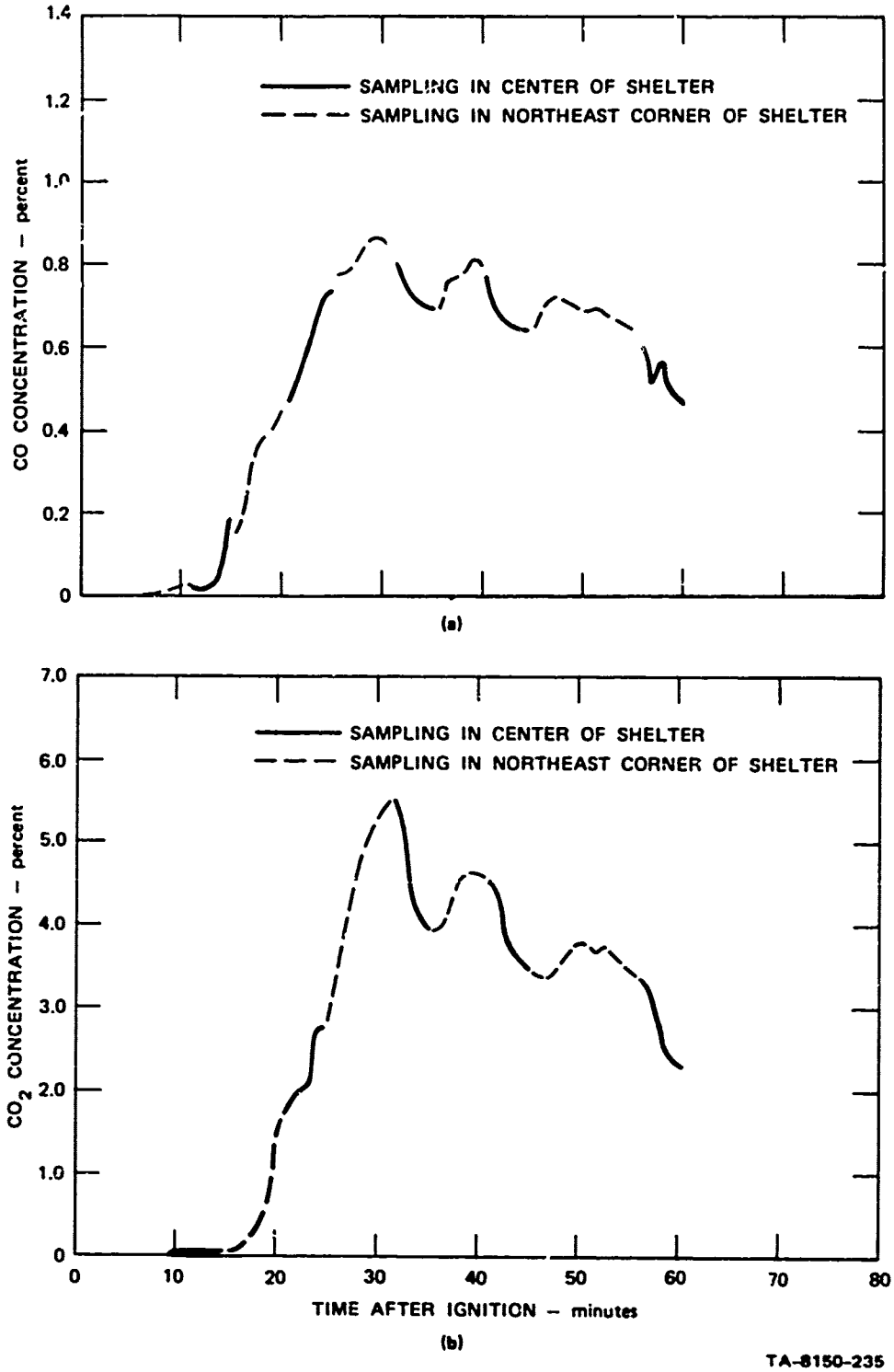

FIGURE E-6 CONCENTRATIONS OF CO AND CO_2 IN SHELTER, CAMP PARKS EXPERIMENT 14

Table E-2

FIRE SPREAD IN BUILDING, CAMP PARKS EXPERIMENT 14

Room Number	Time After Ignition of Room Flashover (minutes)
1	7
2	2
3	13
4	10
5	14
6	10
7	13
8	13

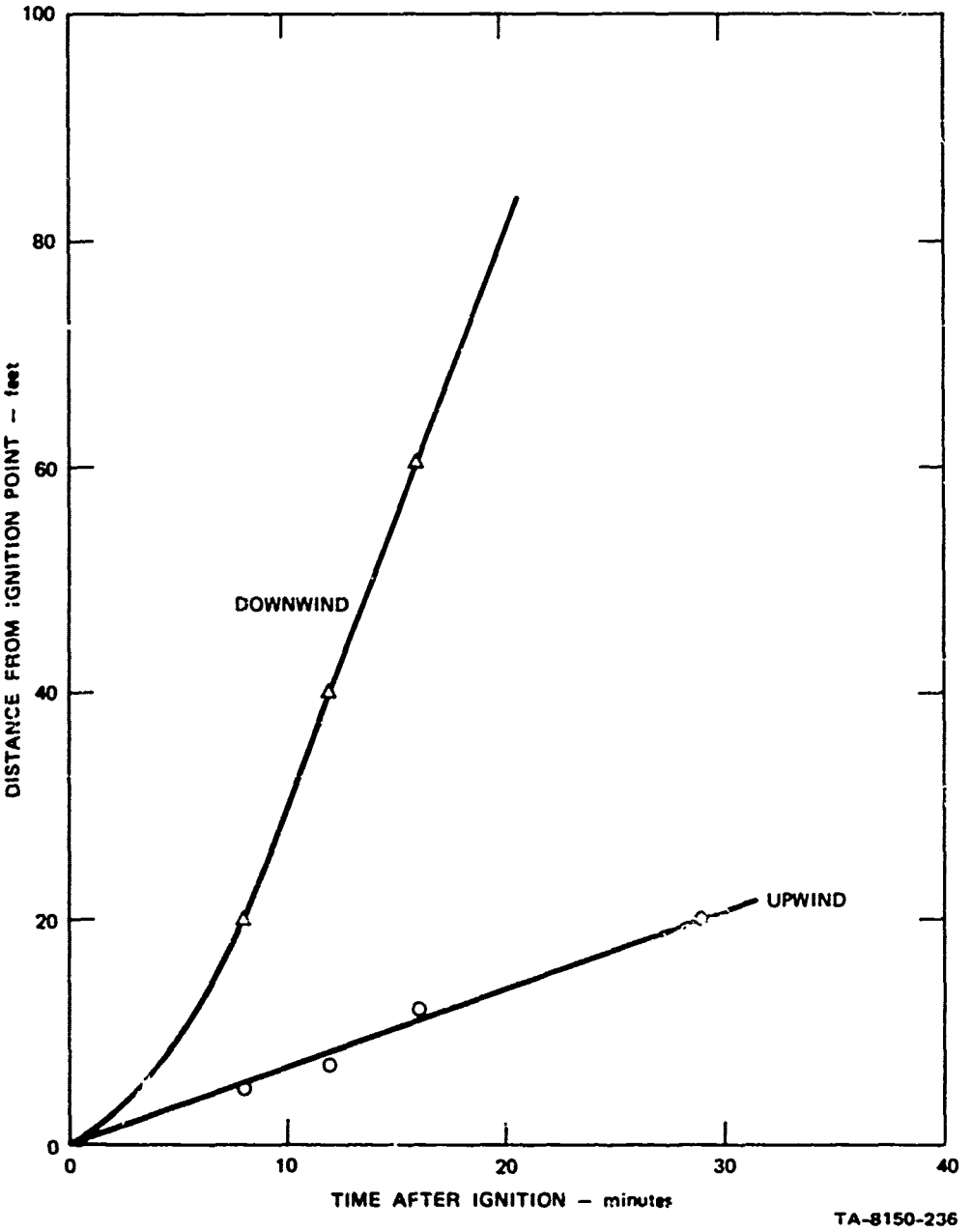

FIGURE E-7 UPWIND AND DOWNWIND FIRE SPREAD IN DEBRIS, CAMP PARKS EXPERIMENT 15

Appendix F

THE FIRE HAZARD CREATED BY FROST-KILLED EUCALYPTUS TREES IN THE EAST BAY HILLS

By

Norman J. Alvares

Appendix F

THE FIRE HAZARD CREATED BY FROST-KILLED EUCALYPTUS TREES IN THE EAST BAY HILLS

The freezing weather during the winter of 1972-73 in the San Francisco Bay Area killed huge stands of semitropical trees of the eucalypt family in the East Bay hills. It was estimated that approximately 3 million trees were so affected over an area of about 30 square miles. This condition was heralded as an extreme fire hazard that could result in potential disaster involving not only the homes within the "hills" area, but also structures of the adjacent cities because of the high firebrand potential of eucalyptus trees. DCPA recognized the extent of this problem and authorized SRI to survey the hazard, the proposed governmental action, the implemented countermeasures, and the parameters of any fires that occur in the area. In particular, the following tasks were initiated:

(1) A survey of eucalyptus forest fire parameters from Australian experience.

(2) Liaison with federal, state, and municipal fire prevention and fire-fighting agencies.

(3) Perusal of regional planning for the potential emergency.

(4) Attendance at pertinent regional meetings addressed to cooperative contigency plans.

(5) Collection of news items associated with the potential emergency.

(6) Preparation for postfire surveys and critiques in the event that a fire does in fact occur in the dead eucalyptus stands.

SRI has actively participated in all the above tasks. For example, in the first task we contacted most of the Australian foresters who are concerned with mass fires in eucalyptus forests (principally A. G. McArthur and R. G. Vines). Vines gave a seminar on Australian fire problems at SRI in July 1973. Summaries of information that we collected were

distributed at meetings of the local fire-fighting agencies so that they would understand the extent of fire danger they faced. However, in our literature searches we were unable to locate any information on either the ignitability or relative flammability of eucalyptic fuels; these data apparently do not exist for either live or freeze-killed fuels. To alleviate this gap, we conducted some rough ignition and burning rate experiments on the most likely kindling fuel in this situation: freeze-killed eucalyptus leaves that would be the kindling fuel for any fires.

The experiments were conducted using naturally dried eucalyptus leaves as the experimental control (at the low input thermal energies of these tests, live leaves would neither ignite nor sustain combustion). These data are summarized in Figures F-1 and F-2. Figure F-1 shows the reciprocal time to piloted ignition of the leaves versus the irradiance H (in cal cm^{-2} sec^{-1}) from a quartz lamp thermal radiation source. Piloted ignition was used since this depicts a more natural phenomonon. Also, the irradiated side of the leaves were blackened so that most of the energy would be absorbed and not reflected from the exposed surface. This again is a ploy to approximate nature because organic materials, such as leaves, absorb the thermal energy emitted by flames in the infrared region with high efficiency. Obviously, the freeze-killed leaves ignite more readily than naturally dried leaves at all measured levels of irradiance.

Figure F-2 shows that the burning rate (the amount of fuel consumed per unit of time) is definitely faster for the freeze-killed leaves than for the naturally dried leaves (roughly twice as fast in the uniform mass-loss region). To place these data in perspective to other forest fuels, we sought information on the flammability of common North American forest fuels. Much to our amazement, such information is either nonexistent or obscurely hidden in the literature because we were unable to find any in the time allotted to this task. However, from our past

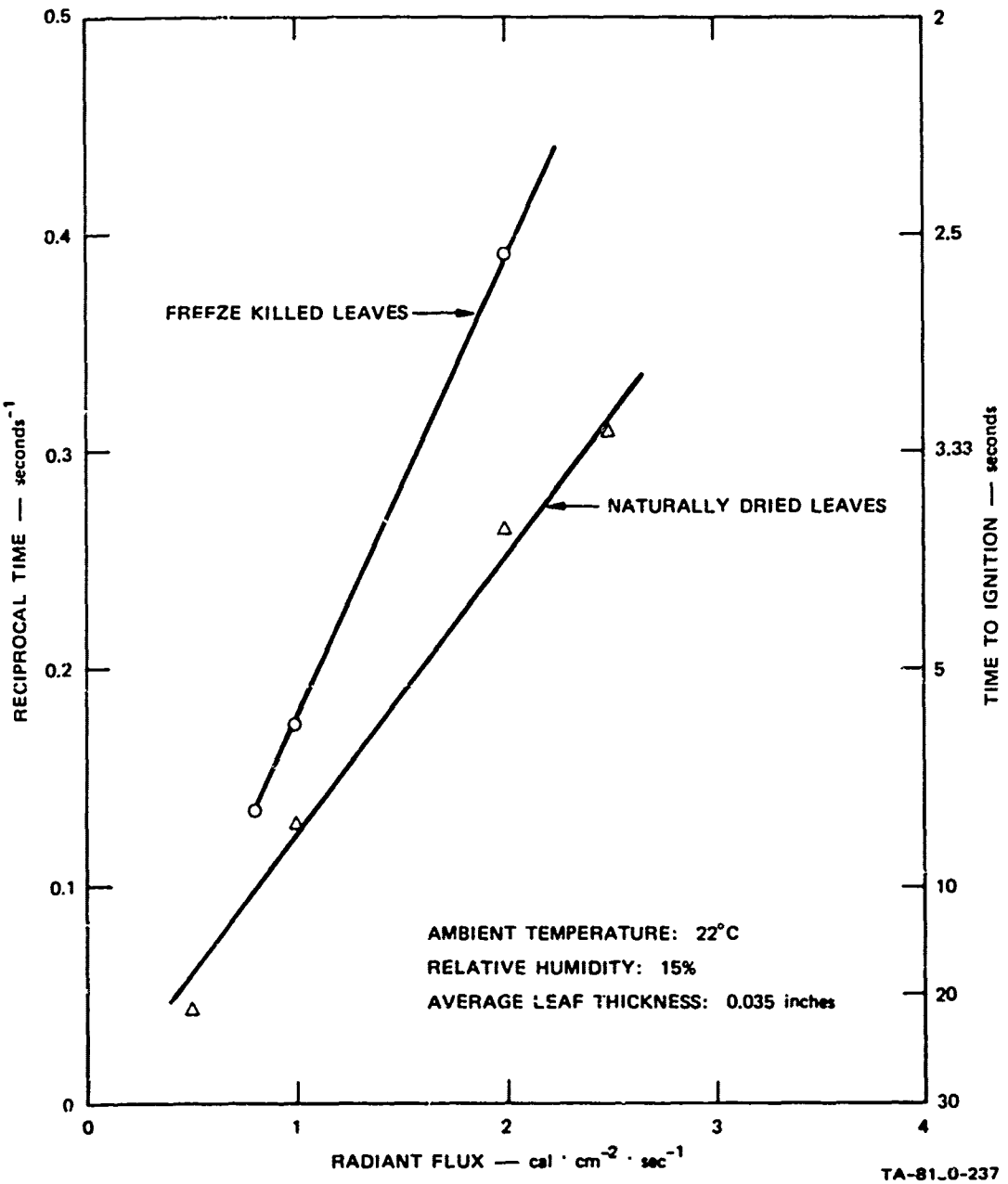

FIGURE F-1 RADIANT IGNITION OF EUCALYPTUS LEAVES

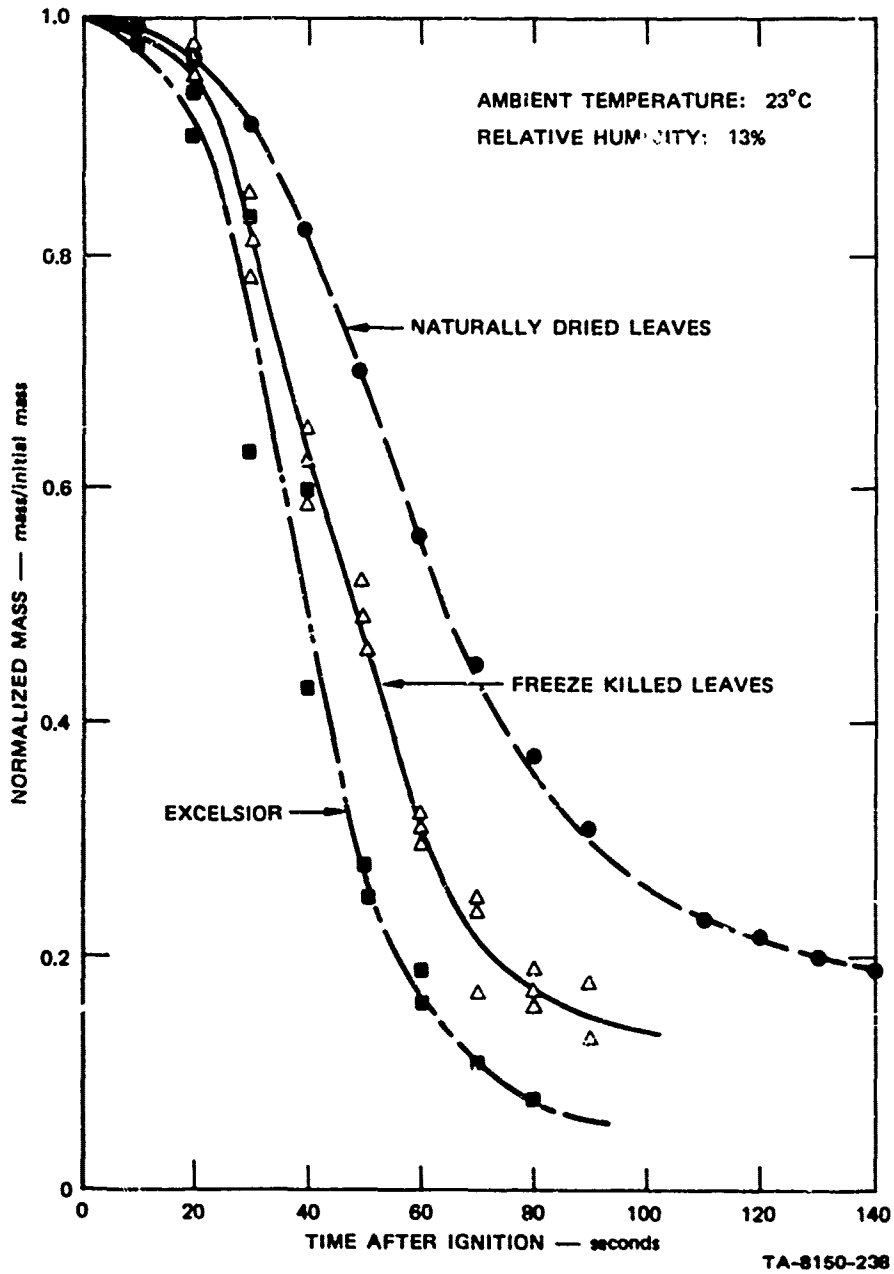

FIGURE F-2 BURNING RATES OF EUCALYPTUS LEAVES

experience in the response of kindling fuels to radiation from atomic weapons, we can place the ignitability and flammability of the freeze-killed eucalyptus leaves in the range of that of single sheets of newspaper.

The accomplishments of the intergovernmental committees have been many. To list a few to date:

(1) Approximately $2.5 million was alloted by the O.E.P. to establish a 100-yard-wide fuel break along the ridge separating the east and west slopes of the affected hills.

(2) Most trees on public lands in the cities have been cleared.

(3) Disposal of the slash has been accomplished with resident "air curtain destructor" furnaces.

(4) A $1 million water storage system and fire mains have been installed by the EBMUD Water Company.

(5) Two new temporary fire stations have been established in the hazard area by the State of California Forest Fire Service.

(6) Permanent and temporary weather stations have been established throughout the ridge area to assess the micrometeorology of the region and to act as early-warning indicators of fire hazard weather.

(7) Evacuation plans and mutual aid assignments have been developed and tested, as have communication codes and equipment standardization.

(8) Roving fire patrols throughout the fire hazard region are scheduled on a daily basis.

(9) Lookout stations are professionally manned during fire danger weather.

(10) A new spirit of cooperation and dialogue has been established in the affected communities so that regional boundaries no longer exist as barriers to communication and cooperative efforts.

During this year of potential crisis, the coordinated efforts of several bay area communities have resulted in cooperative action that can serve to lessen the impact of potential fire disasters. Most of the agencies realize that the threat of mass fires in the urban forest

environment of the East Bay hills is a constantly reoccurring problem that has been brought into focus only because of the added danger from freeze-killed eucalyptus fuels. Thus the real test of this cooperative spirit is whether it endures over the years.

Appendix G

PARTICIPATION IN TWO FIRE EXPERIMENTS

By

C. P. Butler

Appendix G

PARTICIPATION IN TWO FIRE EXPERIMENTS

Opportunities occasionally arise in which techniques and procedures developed to measure the dynamic characteristics of fires in our DCPA Mass Fire Program can be used to characterize the fire environments in other experiments. Our exchange information about techniques and procedures with others has proved to be mutually beneficial. During the past year we took part in two experiments that measured the thermal radiation from different types of fires. This appendix contains descriptions and measurements of the two experiments: prescribed burning for wild land management and fire retardant emulsions to protect "hills" area houses from wildfires. Data and ideas from the latter experiment may prove to be particularly applicable to the nuclear weapon-caused thermal and fire threat to urban areas as a possible countermeasure to protect structures.

1. Thermal Radiation and Carbon Monoxide Concentration Measurements at a Prescribed Wild Lands Fire

a. Description of Experiment

A prescribed burn was conducted in the Palomar District of the Cleveland National Forest in Southern California on May 8, 1973, in an area heavily covered with chaparral. This fire was part of a larger plan of fuel modification to clear areas of heavy brush concentration to:

(1) Reduce public and private losses that result from wildfires and subsequent flooding.

(2) Reduce the burned acreage and the costs of suppressing wildfires.

(3) Save lives of fire fighters and the public.

(4) Increase the amount of forage for domestic livestock.

(5) Improve wildlife habitat.

(6) Improve water yield.

(7) Eliminate present fire closures.

Prescribed burning, as well as hand clearing and clearing with dozers and brush rakes, is one way to accomplish this fuel modification.

The fuel consisted of chamise, mountain mahogany, ceanothus, and manzanita. The brush was about 6 feet high and so dense that it was impossible to walk through. Under the living branches was a 2-foot layer of dead leaves, dried twigs, and broken branches.

The thermal radiation from the fire was measured and those data were compared with data from other tests and other fuels. Carbon monoxide concentrations were measured in the burned over but still smoldering areas that forest fighters commonly work in.

b. Experimental Measurements

A radiometer was placed 100 feet from the fuel's edge so that the radiometer's field of view included 90 feet of the brush field edge. It was possible to view the fuel in this way because a fuel break had been cut through the brush. The flame areas for the same field of view as seen by the radiometer were recorded by motion picture cameras. The brush was ignited along the entire 90-foot edge by several men with hand torches. The radiometer recorded a maximum flux of 1.4 $cal\ cm^{-2}\ min^{-1}$ 6 minutes after ignition. At this time the flame area recorded by the motion picture camera was 900 square feet. The radiant flux to the radiometer continually decreased after 6 minutes as the fire spread away from the radiometer and camera.

The carbon monoxide concentration in the air 5 feet above the burned-over ground was measured with Draeger tubes. The carbon monoxide was produced primarily from glowing fragments of leaves and tiny twigs that smoldered 50 to 55 minutes after the fire front had passed. The sampling area was selected by an experienced forester as a typical environment in which forest fire fighters are required to work for hours at a time. The gaseous irritants were of sufficient quantity to cause eye and nose irritation. The carbon monoxide concentration was measured at 10 ppm.

c. Conclusions

The emittance of the flames of the brush fire can be calculated by comparing the measured irradiance and flame area of the fire with those of a "standard" fire whose irradiation, flame area, and emittance are known. If the flame temperatures of the standard and brushfires are assumed to be equal and if the configuration factors (which designate the fraction of the radiation leaving the source that arrives at the receiver) are assumed to be directly proportional to the flame area, then the emittance of the brush fire flames is:

$$\varepsilon = \frac{H \varepsilon_o A_o}{H_o A} ,$$

where ε_o, A_o, and H_o are the emittance, flame area, and irradiance of the standard fire, respectively, and A and H are the flame area and irradiance of the brush fire. Data from the Camp Parks structural fires were used as the standard fires. In these fires,[1] the emittance is known to be almost unity and the average irradiance is 3.2 cal cm^{-2} min^{-1} for a flame area of 620 square feet. Therefore the calculated emittance of the brush fire flames is 0.3.

Several experienced forest fire fighters have died because they acted irrationally. Their coworkers[2] made statements like, "I wonder why he did that; he knew better. I just can't understand." So the question was asked. "Could the fire fighter's judgment have been impaired because of the physiological effect of carbon monoxide?" The measured concentration of carbon monoxide of 10 ppm is about an order of magnitude below the allowable exposure for several hours for any toxic physiological response.[3] Therefore, it is unlikely that carbon monoxide alone was responsible for the seemingly impaired judgment of the fire fighters.

2. A Fire Retardant Emulsion to Protect Hills-Area Structures from Wildfires

a. Description of Experiment

A water-oil emulsion fire retardant was tested on July 27, 1973, by the Palo Alto Fire Department. The purpose of the test was to determine if this emulsion, when sprayed on a wooden house, would protect the structure from the fire of a nearby brush fire.

The structure used in the test was a 10-by 10-feet shack with exterior grade plywood siding and a cedar shingle roof. Chamise brush was placed 10 feet from the structure on two sides. The brush was piled 6 feet high and about 6 feet wide.

Petrolite water-oil emulsion was sprayed on the exterior structure surfaces so that approximately a 1/4-inch-thick layer adhered to the surfaces. The brush was ignited about 15 minutes after the emulsion was applied; the response of the structure to the fire was observed throughout the fire.

b. Experimental Measurements

The thermal radiation was measured at a distance of 100 feet from the burning brush. A maximum radiant flux of 0.6 cal cm^{-2} min^{-1} was measured. From this measurement the maximum radiant flux to the exterior surfaces of the structure, which were protected by the emulsion, was crudely estimated to be 60 cal cm^{-2} min^{-1}.

At no time during the 20-minute brush fire were flames observed from the exterior plywood siding. However, a few flames were seen in the protruding cedar shingles at the edge of the roof where flames from the brush fire had actually been blown so that they touched the roof. The walls showed considerable charring and the heat broke the window.

c. Conclusions

The test demonstrated that the emulsion was a very effective fire retardant for wood buildings exposed to brush fires. It had previously been shown[1] that radiant fluxes of 30 cal cm^{-2} min^{-1} for 5 minutes would ignite both redwood siding and particle board. The plywood siding without the emulsion coating would probably ignite as easily as redwood siding or particle board, but with the emulsion coating it withstood radiant fluxes much higher than 30 cal cm^{-2} min^{-1}.

The emulsion coating will adhere to vertical surfaces for several hours and thus will provide protection against a fire threat for some length of time. It may be an effective countermeasure against a nuclear weapon-caused, thermal and fire threat to structures.

REFERENCES

1. S.J. Wiersma and S.B. Martin, "Measurements of the Dynamics of Structural Fires," OCD Work Unit 2561A, Annual Report, Project PYU 8150, Stanford Research Institute, Menlo Park, California August 1971).

2. Private Communication with T.E. Lundgren, Supervisory Forestry Technician, U.S.D.A., Forest Service, Escondido, California.

3. R.E. Reinke and C.F. Reinhardt, Modern Plastics, Vol. 50, No. 2, p. 94 (February 1973).